Nonlinear Observer Design and Strapdown Inertial Navigation Systems for Unmanned Aerial Vehicles

Professor Thor I. Fossen

Department of Engineering Cybernetics
NTNU Centre for Autonomous Marine Operations and Systems
Norwegian University of Science and Technology (NTNU)

NTNU is the largest of the eight universities in Norway (located in the cities Trondheim, Ålesund and Gjøvik).
(9 faculties, 54 departments, 39 700 students, 4377 academic/scientific employees)

Joint work with…

Professor Tor Arne Johansen
NTNU Norwegian University of Science and Technology

Dr. Håvard Fjær Grip
NASA JPL, Pasadena, CA

Adjunct Associate Professor Nadia Sokolova
NTNU Norwegian University of Science and Technology

Professor Ali Saberi
Washington State University

Dr. Jakob Mahler Hansen
NTNU Norwegian University of Science and Technology

Dr. Torleiv H. Bryne
NTNU Norwegian University of Science and Technology

Outline

Motivation

Nonlinear Observer Design for Robust Autonomous Navigation

- Attitude representations and global stability on SO(3)
- Nonlinear attitude observers
- Core Algorithm for Nonlinear Strapdown INS:
  Feedback interconnection of the attitude and translational motion (TMO) observers
- The *eXogenous Kalman fiter (XKF)* for optimal handling of noise when using nonlinear observers

Applications

Unmanned Aerial Vehicles (UAVs)

- Strapdown INS aided by GNSS and camera measurements (optical flow)
- Autonomous landing onboard ships

Concluding Remarks

Motivation

Inertial Navigation Systems (INS) and Global Navigation Satellite Systems (GNSS) are used in manned and unmanned vehicles. Robust navigation is very important when designing automatic/autonomous systems.

Why not buy an integrated INS and GNSS system?

- High-quality systems are expensive
- You cannot modify the SW (proprietary code). Non-trivial to add SW for failure detection, fault tolerance etc. which is necessary for robust navigation and tight integration with the autopilot.
- Sensor fusion with other sensors is difficult (no access to Kalman filter source code)

Why use nonlinear observes instead of the well-proven extended Kalman filter (EKF)?

- A small computational footprint is important in embedded systems with limited power. The EKF uses hundreds of Riccati equations, which can be avoided.
- Explicit stability requirements for semiglobal or global exponential stability (not available when using the EKF). This gives robustness guarantees and tuning rules for the convergence rate of the estimates.

What is an Inertial Navigation System?

An instrument (electronic + sensors) which is using its initial state (position) and internal motion sensors (gyroscopes + accelerometers) to measure and calculate its subsequent positions in space with high accuracy, stability and update rate.

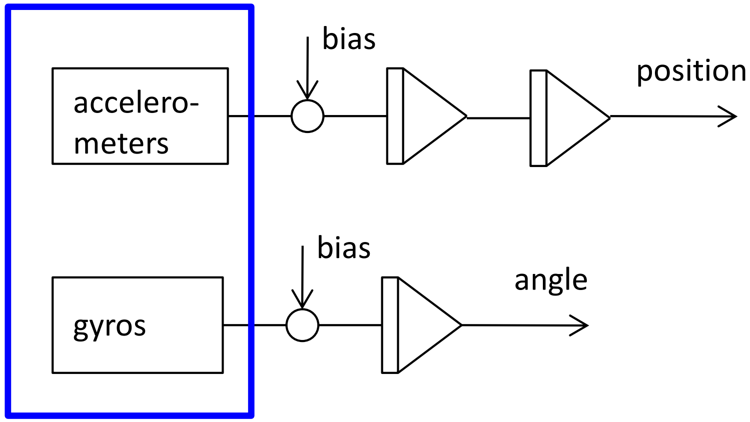

Inertial measurement unit (IMU)

The integrated signals will drift. Hence, the system must be aided by GNSS, hydroacoustic positioning reference (HPR) systems or other reference systems.

The sensors can be mounted on a gimbal or a moving body (strapdown), which is related to the North-East-Down positions by the navigation differential equations.

The Sensonor STIM 300 IMU

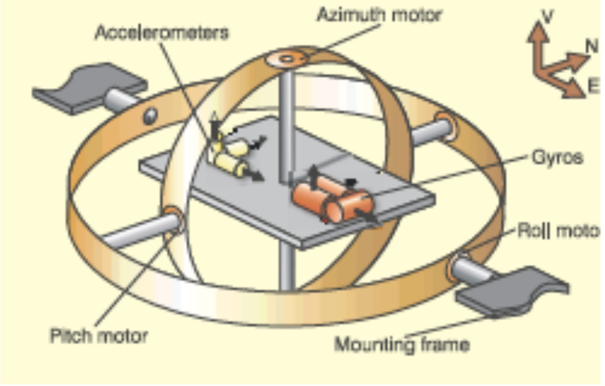

Inertial Navigation Systems – History

- 1944 German V2 combined two gyroscopes and a lateral accelerometer with a analog computer to adjust the azimuth for the rocket in flight
- 1950's Atlas ICBM
- 1958 USS Nautilus to North Pole
- 1960 The "Kalman Filter" is invented
- 1961 Apollo program
- 1969 Commercial Navigation Boeing 747

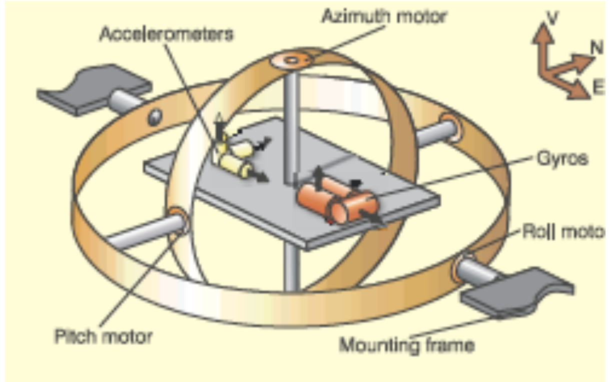

Today gimbaled systems are replaced by strapdown INS

- 1980's Practical ring laser gyro systems and strapdown INS using fast computers (Strapdown INS runs at 2 000 Hz)
- 1985 Development of fiber optic gyros (FOGs) starts
- 1990s Low-cost MEMS gyros and accelerometers
- 2006 The Mahoney, Hamel and Pflimlin nonlinear attitude observer can replace the extended Kalman filter (EKF) and stability is proven
- 2012-2016 A nonlinear observer framework for strapdown INS (attitude and translational motion) is developed at NTNU. Tailor-made for embedded computers and autonomous vehicles with limited computational capacity.
- 2017 The eXogenous Kalman filter (XKF) adds optimality and covariance estimates for nonlinear observers.

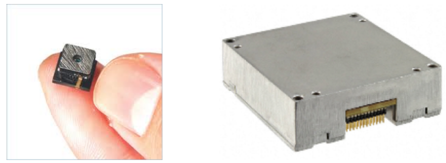

State Estimator (Observer) – Inverse Problem

The ultimate goal of a state estimator or an observer is to reconstruct the unmeasured state vector **x** from the measurements **u** and **y** of a dynamical system given by ordinary differential equations (ODEs). This only works if the system is observable.

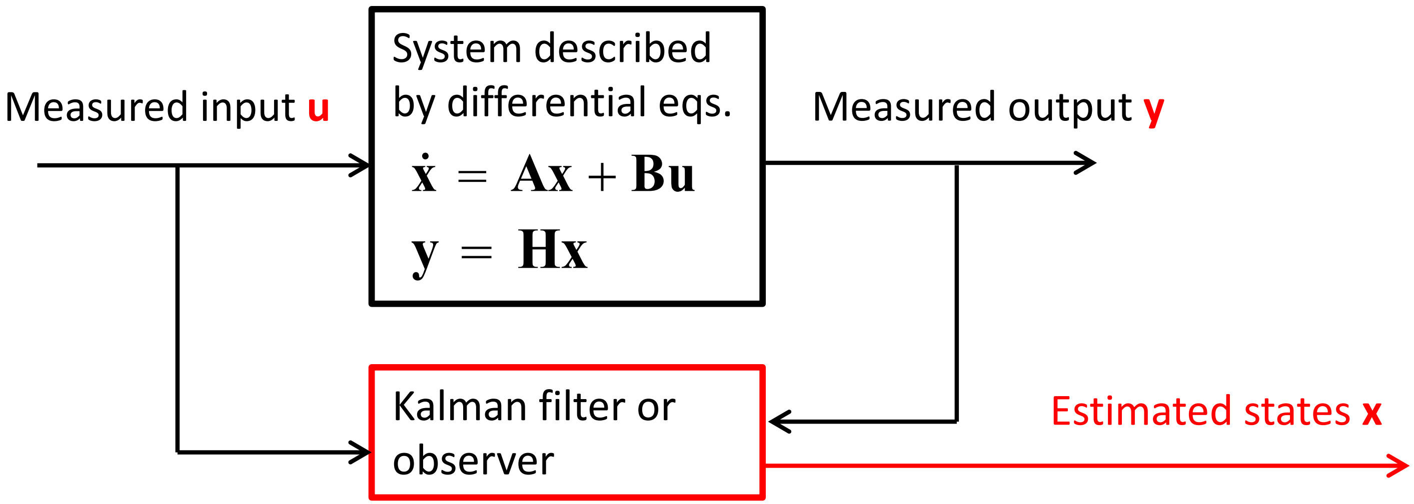

Some observations:

It is possible to estimate linear velocity and acceleration from a position sensor:

- Signal-based approach (no input **u**). This is equivalent to differentiating the measured position **y**
- Acceleration as input **u** and a double-integrator model improves the performance
- Alternatively the vehicle model can be used to compute acceleration.
  Drawback: model parameters must be known

Why should we use alternatives to the well-celebrated Kalman Filter?

Since 1960 the Kalman filter, and nonlinear extensions thereof, has been used to provide integrated navigation solutions based on different types of measurements.

The Kalman filter is used in millions of applications and it is the core algorithm of all modern navigation systems.

Rudolf Kalman (May 19, 1930 – July 2, 2016)

However,

- Nonlinear observers provide explicit stability and robustness guarantees that are typically not available for nonlinear Kalman filter implementations.
- The number of C-code lines can be significantly reduced. This simplifies documentation and maintenance.
- Tuning and commissioning are less time consuming.
- MEMS technology and faster computers make it possible to replace gimbaled mechanical solutions with strapdown navigation differential equations running at 100-2000 Hz.

50th anniversary of the Kalman filter in 2010

Kalman, R. E. (1960). "Contributions to the theory of optimal control". Bol. Soc. Mat. Mexicana.
Kalman, R.E. (1960). "A new approach to linear filtering and prediction problems" (PDF). Journal of Basic Engineering. 82 (1): 35–45
Kalman, R.E.; Bucy, R.S. (1961). "New Results in Linear Filtering and Prediction Theory". Journal of Basic Engineering. March 1961.

Nonlinear Attitude Estimation

The key component of strapdown INS

Attitude Representations

Coordinate systems for local navigation:

BODY – body-fixed frame

NED – North-East-Down frame is approximated as the inertial frame by neglecting the Earth rotation and movement of the Earth in the solar system

Attitude can be described by a 3 x 3 matrix (9-elements) relating a vector in BODY to a vector in NED

Consequently, a NED vector $\mathbf{v}^n$ is related to a BODY vector $\mathbf{v}^b$ by the rotation matrix according to

$$\boxed{\mathbf{v}^n = \mathbf{R}\mathbf{v}^b \quad \text{where} \quad \mathbf{R} \text{ on } SO(3)}$$

O(3) is the group of all orthogonal matrices, i.e. $\mathbf{R}\mathbf{R}^T = \mathbf{I}_3$ and $\mathbf{R}^T = \mathbf{R}^{-1}$

SO(3) special orthogonal group.
The subgroup of the O(3) satisfying:
$\det(\mathbf{R}) = 1$

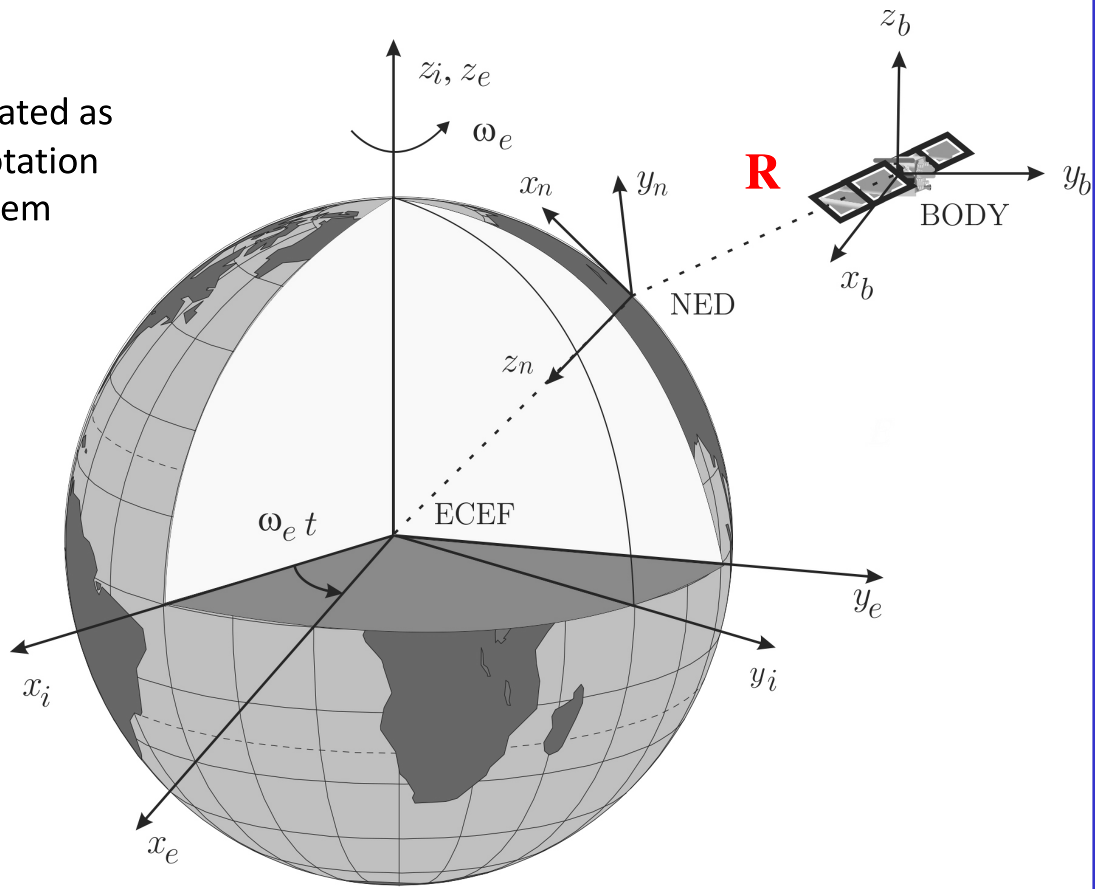

Attitude from Reference Vectors

The main challenge in many navigation problems is the estimation of attitude, represented as the rotation of a body-fixed coordinate frame with respect to some reference frame.

- The attitude can be estimated by comparing a set of vectors measured in the BODY frame using accelerometers, magnetometers or sun sensors with a set of reference vectors in a second reference frame usually NED.

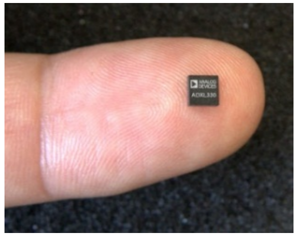

Micro-electro-mechanical system (MEMS) accelerometer technology capable of tracking vibrations in industrial equipment at frequencies as high as 22 kHz. Analog Devices (2008)

- Algorithms such as QUEST and TRIAD (Shuster and Oh, 1981) can be used to determine the attitude algebraically from vector measurements if at least two pairs of nonparallel vectors are available.

- However, vector measurements are typically affected by noise. This suggests that an observer based on a dynamic model and rate gyroscopes should be used to obtain accurate attitude information at high frequencies for accelerated vehicles.

- Gyro measurements are subject to bias, which must be estimated along with the attitude.

M. D. Shuster and S. D. Oh (1981). Three-axis attitude determination from vector observations, Journal of Guidance, Control and Dynamics, vol. 4, no. 1, pp. 70–77.

Parameterizations on SO(3)

3-parameter representation (Euler Angles)

$$\mathbf{R}_b^n(\Theta_{nb}) = \begin{bmatrix} c\psi c\theta & -s\psi c\phi + c\psi s\theta s\phi & s\psi s\phi + c\psi c\phi s\theta \\ s\psi c\theta & c\psi c\phi + s\phi s\theta s\psi & -c\psi s\phi + s\theta s\psi c\phi \\ -s\theta & c\theta s\phi & c\theta c\phi \end{bmatrix}$$

$$\begin{aligned} \dot{\phi} &= p + q\sin\phi\tan\theta + r\cos\phi\tan\theta \\ \dot{\theta} &= q\cos\phi - r\sin\phi \\ \dot{\psi} &= q\frac{\sin\phi}{\cos\theta} + r\frac{\cos\phi}{\cos\theta}, \quad \theta \neq \pm 90^o \end{aligned}$$

- This representation is singular for 90 degrees pitch
- Only <u>local</u> exponential or asymptotically stable observers can be designed

4-parameter representation (Quaternions)

$$\mathbf{R}_b^n(\mathbf{q}) = \begin{bmatrix} 1-2(\varepsilon_2^2+\varepsilon_3^2) & 2(\varepsilon_1\varepsilon_2 - \varepsilon_3\eta) & 2(\varepsilon_1\varepsilon_3 + \varepsilon_2\eta) \\ 2(\varepsilon_1\varepsilon_2 + \varepsilon_3\eta) & 1-2(\varepsilon_1^2+\varepsilon_3^2) & 2(\varepsilon_2\varepsilon_3 - \varepsilon_1\eta) \\ 2(\varepsilon_1\varepsilon_3 - \varepsilon_2\eta) & 2(\varepsilon_2\varepsilon_3 + \varepsilon_1\eta) & 1-2(\varepsilon_1^2+\varepsilon_2^2) \end{bmatrix}$$

$$\begin{aligned} \dot{\eta} &= -\frac{1}{2}(\varepsilon_1 p + \varepsilon_2 q + \varepsilon_3 r) \\ \dot{\varepsilon}_1 &= \frac{1}{2}(\eta p - \varepsilon_3 q + \varepsilon_2 r) \\ \dot{\varepsilon}_2 &= \frac{1}{2}(\varepsilon_3 p + \eta q - \varepsilon_1 r) \\ \dot{\varepsilon}_3 &= \frac{1}{2}(-\varepsilon_2 p + \varepsilon_1 q + \eta r) \end{aligned}$$

- Avoids the singularity by using one extra parameter
- Two equilibrium points corresponding to $\eta = 1$ or $\eta = -1$
- <u>Almost-global</u> or <u>semiglobal</u> exponential stability can be achieved

Kinematic constraint:

$$\eta^2 + \varepsilon_1^2 + \varepsilon_2^2 + \varepsilon_3^2 = 1$$

It is impossible to obtain global attitude for Euler angles.
Quaternions can be globally stabilized using discontinuous feedback.

Topological Obstructions

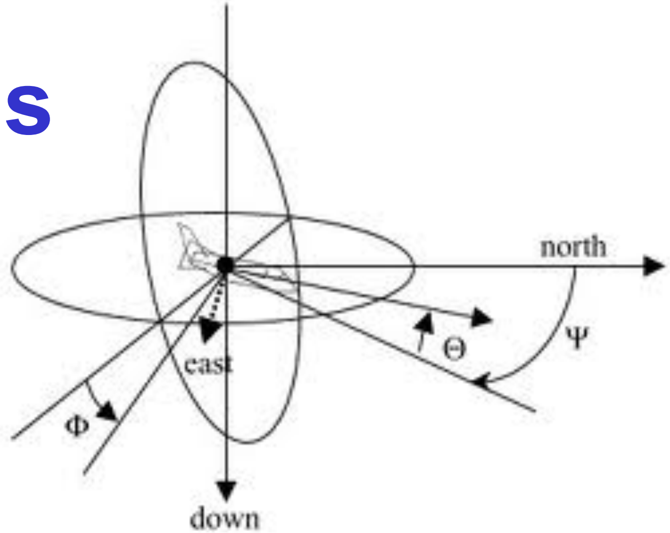

Attitude is usually represented by:

- Euler angles
- Quaternions on the unit sphere
- Rotation matrix on SO(3)

Topological obstructions prevent global asymptotic stability results, unless discontinuities are introduced in the dynamics (Bhat and Bernstein, 2000). Results such as semiglobal or almost-global stability are therefore common, with a vanishing convergence rate in the vicinity of estimation errors representing a 180° rotation.

S. P. Bhat and D. S. Bernstein (2000). A topological obstruction to continuous global stabilization of rotational motion and the unwinding phenomenon, *Systems and Control Letter*, vol. 39, pp. 63–70.

The topological obstructions to global stability can be avoided if one does not restrict the estimated attitude to the unit sphere or SO(3), for instance by estimating a 3x3 matrix with 9 elements that converges to a rotation matrix on SO(3).

The “*Attitude Observer*” and “*Translation Motion Observer*” (TMO)

Σ_1 – The attitude observer typically runs at 100-1000 Hz and it uses accelerometers and magnetometers to compute one of the following:

- Unit quaternions
- Roll, pitch and yaw angles
- Rotation matrix

Σ_2 – The translational motion observer (TMO) estimates position, linear velocity and linear acceleration (specific force). Typical update rate is 1-10 HZ for GNSS-aided systems.

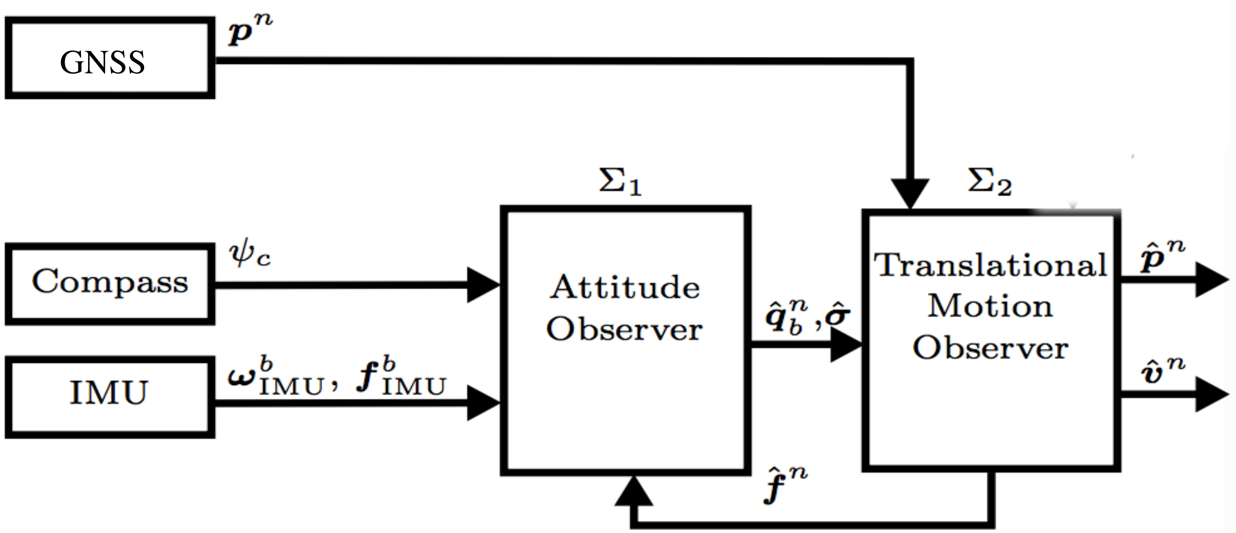

Feedback interconnection of the attitude and TMO observers.

Nonlinear Attitude Estimation

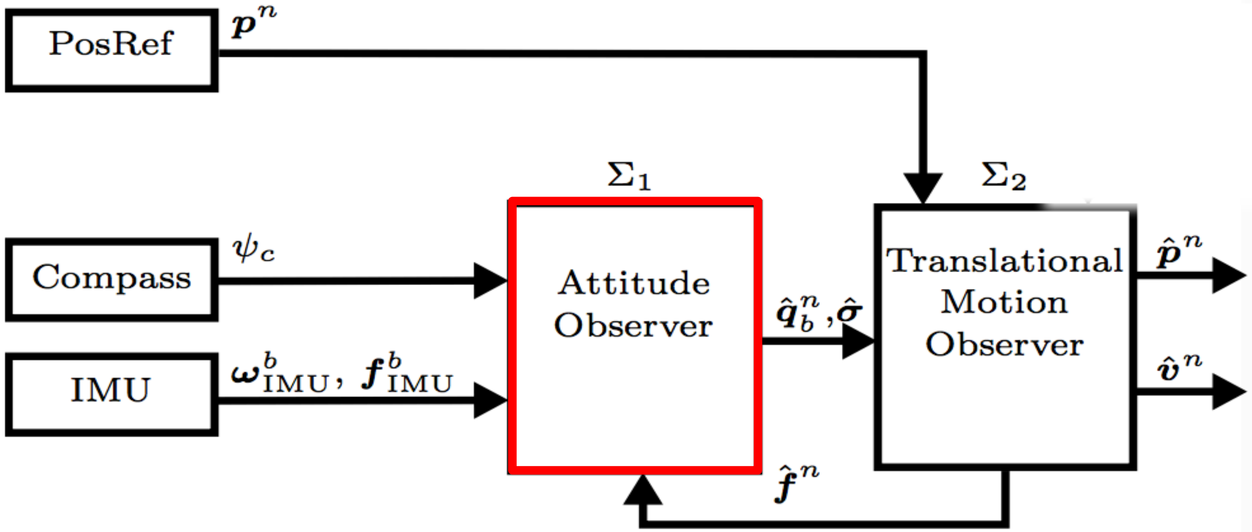

Feedback interconnection where the specific force f^n is estimated. Important for highly accelerated vehicles.

$$\mathbf{f^n} = \mathbf{R}(\dot{\mathbf{v}}^\mathbf{b} + \omega^\mathbf{b} \times \mathbf{v}^\mathbf{b}) - \mathbf{g^n}$$
$$\dot{\mathbf{v}}^n = \mathbf{R}(\dot{\mathbf{v}}^\mathbf{b} + \omega^\mathbf{b} \times \mathbf{v}^\mathbf{b})$$

Reference vectors (BODY):
- Magnetic field: $\boldsymbol{m}^b$
- Acceleration/specific force: $\mathbf{f}^b$
- Optical flow: $\boldsymbol{v}^b$

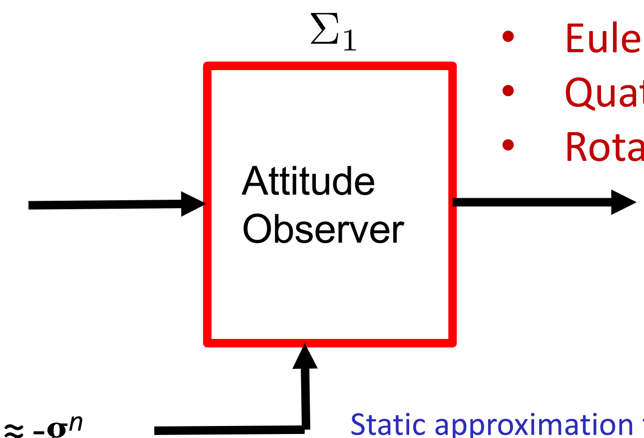

- Euler angles
- Quaternions on the unit sphere
- Rotation matrix on SO(3)

Reference vectors (NED):
- Magnetic field: $\boldsymbol{m}^n$
- Acceleration/specific force: $\mathbf{f}^n \approx -\mathbf{g}^n$
- GNSS speed: $\boldsymbol{v}^n$

Static approximation for non-accelerated vehicles

Nonlinear Attitude Observer

Quaternion representation

$$\Sigma_1 : \begin{cases} \dot{\hat{\boldsymbol{q}}}_b^n = \boldsymbol{T}(\hat{\boldsymbol{q}}_b^n)(\boldsymbol{\omega}_{b/n,\mathrm{IMU}}^b - \hat{\boldsymbol{b}}_g^b + \hat{\boldsymbol{\sigma}}) \\ \dot{\hat{\boldsymbol{b}}}_g^b = \mathrm{Proj}(\hat{\boldsymbol{b}}_g^b, -k_I \hat{\boldsymbol{\sigma}}) \end{cases}$$

Injection term:

$$\hat{\boldsymbol{\sigma}} = k_1 \boldsymbol{c}^b \times \boldsymbol{R}(\hat{\boldsymbol{q}}_b^n)^\intercal \boldsymbol{c}^n + k_2 \boldsymbol{f}_{\mathrm{IMU}}^b \times \boldsymbol{R}(\hat{\boldsymbol{q}}_b^n)^\intercal \hat{\boldsymbol{f}}^n$$

Injection term based on compass and specific force measurements, alternatively other reference vectors.

Rotation matrix representation

$$\dot{\hat{R}} = \hat{R}S(\omega_{\mathrm{m}}^{\mathrm{b}} - \hat{b}) + \boldsymbol{\sigma} K_P J(t, \hat{R}),$$
$$\dot{\hat{b}} = \mathrm{Proj}(\hat{b}, -k_I \,\mathrm{vex}(\mathbb{P}_{\mathrm{a}}(\hat{R}_{\mathrm{s}}' K_P J(t, \hat{R}))))$$

Convert estimates to be on SO(3)

$$\bar{R}(\hat{R}) = \left[\bar{r}_1 \;\; \bar{r}_2 \;\; S(\bar{r}_1)\bar{r}_2\right],$$
$$\bar{r}_1 = \hat{r}_1 / \max\{\|\hat{r}_1\|, \mu\},$$
$$\bar{r}_2 = (I_3 - \bar{r}_1\bar{r}_1')\hat{r}_2 / \max\{\|(I_3 - \bar{r}_1\bar{r}_1')\hat{r}_2\|, \mu\}$$

Quaternions give a semiglobal result, while estimation of the 9 elements in the rotation matrix gives GES.

- **Mahoney, R., Hamel , T. and Pflimlin, J.M. (2008).** Nonlinear complementary filters on the special orthogonal group. *IEEE Trans. Automatic Control* 53(5), 1203–2018
- **Grip, T.H., Fossen, T.I, Johansen, T.A. and Saberi, A.(2012).** Attitude estimation using biased gyro and vector measurements with time-varying reference vectors. *IEEE Trans. Automatic Control* 57(5), 1332–1338
- **Grip, H. F., T. I. Fossen, T. A. Johansen and A. Saberi (2015).** Globally Exponentially Stable Attitude and Gyro Bias Estimation with Application to GNSS/INS Integration. *Automatica*. Volume 51, Pages 158–166.
- **Grip, T.H., Fossen, T.I, Johansen, T.A. and Saberi, A.(2013).** Nonlinear Observer for GNSS-Aided Inertial Navigation with Quaternion-Based Attitude Estimation. In *Proc. of the American Control Conference,* 272–279

The Attitude Estimation Problem: Remarks on Global Stability on SO(3)

Euler angle representation

- It is impossible to obtain global results when using Euler angles due to the representation singularity.

Unit Quaternion representation

- **The quaternion attitude observer results in semiglobal stability (it is not global due to several equilibria).**

  However, it is possible to achieve global results through introduction of discontinuities to avoid the topological obstruction and thus get one equilibrium point.

Rotation matrix representation

- **When estimating the 9 elements of the matrix $\mathbf{R}$ (over-parameterized estimation problem) the origin is GES on $\mathbb{R}^{3x3}$.**

  The SO(3) property cannot be forced on the system – *structural limitation of SO(3)* – since this kill the observer7convergence properties. Hence, the estimates are on $\mathbb{R}^{3x3}$ and not on SO(3).

  BUT, the estimate of $\mathbf{R}$ on $\mathbb{R}^{3x3}$ converge to SO(3) asymptotically. Even better, we can convert the estimates to SO(3) at each time sample to improve transient behavior.

Core Algorithm for Nonlinear Strapdown INS

Integrated Navigation

When integrating acceleration and angular rates the solutions will drift due to measurement noise and bias terms. An integrated navigation system is a navigation system, which is aided by one or more position reference (PosRef) systems such as:

- GNSS (GPS, Glonass, Galileo, BeiDou)
- Hydro-acoustic positioning reference (HPR) systems
- Machine vision (optical camera)

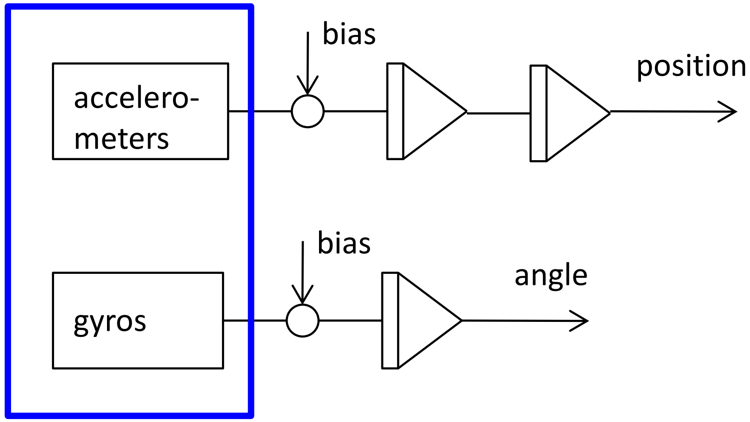

Inertial measurement unit (IMU)

The resulting system is a feedback interconnection of two observers for attitude and translational motions

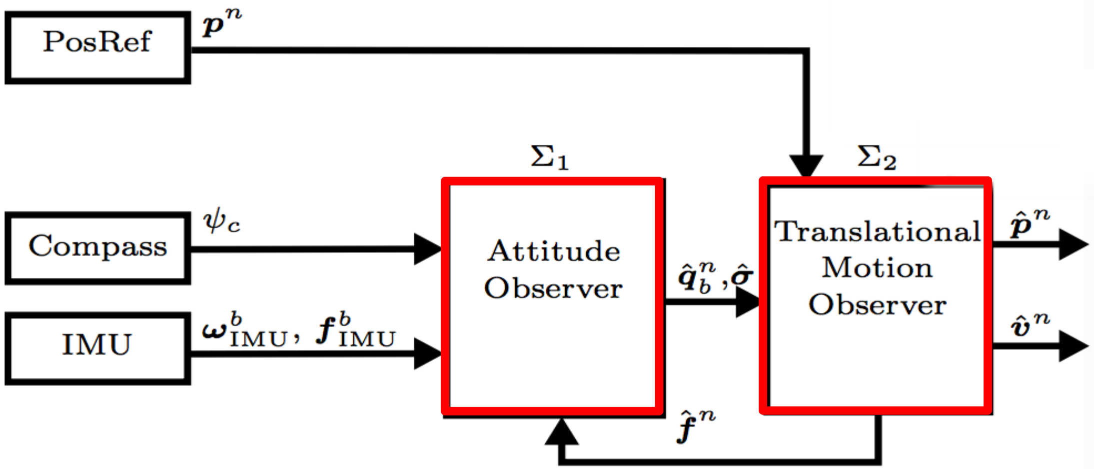

Dead reckoning is referred to as the case when the PosRef systems fail and position and linear velocity are predicted using the observers without PosRef updates.

GES Attitude and TMO Observers – Rotation Matrix Representation

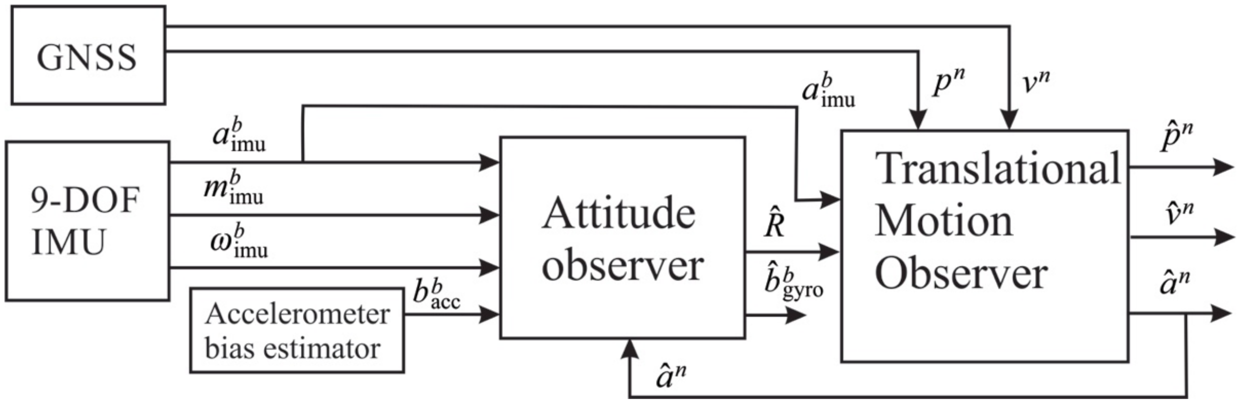

Attitude Observer

$$\dot{\hat{R}} = \hat{R}S(\omega^{\mathrm{b}}_{\mathrm{m}} - \hat{b}) + \sigma K_P J(t,\hat{R}),$$
$$\dot{\hat{b}} = \mathrm{Proj}(\hat{b}, -k_I \,\mathrm{vex}(\mathbb{P}_{\mathrm{a}}(\hat{R}_{\mathrm{s}}' K_P J(t,\hat{R}))))$$

Nonlinear Injection Term

$$J(a^{\mathrm{b}}, a^{\mathrm{n}}, m^{\mathrm{b}}, m^{\mathrm{n}}, \hat{R}) = A_{\mathrm{n}} A_{\mathrm{b}}' - \hat{R} A_{\mathrm{b}} A_{\mathrm{b}}',$$
$$A_{\mathrm{b}} = \left[m^{\mathrm{b}} \quad m^{\mathrm{b}} \times a^{\mathrm{b}} \quad m^{\mathrm{b}} \times (m^{\mathrm{b}} \times a^{\mathrm{b}}) \right]$$
$$A_{\mathrm{n}} = \left[m^{\mathrm{n}} \quad m^{\mathrm{n}} \times a^{\mathrm{n}} \quad m^{\mathrm{n}} \times (m^{\mathrm{n}} \times a^{\mathrm{n}}) \right]$$

Translational Motion Observer (NED)

$$\dot{\hat{p}}^{\mathrm{n}} = \hat{v}^{\mathrm{n}} + K_{pp}(p^{\mathrm{n}} - \hat{p}^{\mathrm{n}}) + K_{pv}(v^{\mathrm{n}}_{\mathrm{m}} - C_v \hat{v}^{\mathrm{n}}),$$
$$\dot{\hat{v}}^{\mathrm{n}} = \hat{a}^{\mathrm{n}} + g^{\mathrm{n}} + K_{vp}(p^{\mathrm{n}} - \hat{p}^{\mathrm{n}}) + K_{vv}(v^{\mathrm{n}}_{\mathrm{m}} - C_v \hat{v}^{\mathrm{n}}),$$
$$\dot{\xi} = -\sigma K_P \hat{J} a^{\mathrm{b}} + K_{\xi p}(p^{\mathrm{n}} - \hat{p}^{\mathrm{n}}) + K_{\xi v}(v^{\mathrm{n}}_{\mathrm{m}} - C_v \hat{v}^{\mathrm{n}})$$
$$\hat{a}^{\mathrm{n}} = \hat{R} a^{\mathrm{b}} + \xi,$$

$$\bar{R}(\hat{R}) = \left[\bar{r}_1 \;\; \bar{r}_2 \;\; S(\bar{r}_1)\bar{r}_2 \right],$$
$$\bar{r}_1 = \hat{r}_1 / \max\{\|\hat{r}_1\|, \mu\},$$
$$\bar{r}_2 = (I_3 - \bar{r}_1 \bar{r}_1')\hat{r}_2 / \max\{\|(I_3 - \bar{r}_1 \bar{r}_1')\hat{r}_2\|, \mu\}$$

Grip, H. F., T. I. Fossen, T. A. Johansen and A. Saberi. Attitude Estimation Using Biased Gyro and Vector Measurements with Time-Varying Reference Vector. *IEEE Transactions on Automatic Control*, Vol. 57, No. 5, pp. 1332-1338, May 2012
Grip, H. F., T. I. Fossen, T. A. Johansen and A. Saberi. A Nonlinear Observer for Integration of GNSS and IMU Measurements with Gyro Bias Estimation, *Proc. of the ACC'12*, Montreal, Canada, 24-27 March 2012.

Semiglobal Exponential Stable Attitude and TMO Observers – Unit Quaternion Representation

Translational Motion Observer (ECEF)

$$
\begin{aligned}
\dot{\hat{p}}^{\mathrm{e}} &= \hat{v}^{\mathrm{e}} + \theta K_{pp}(p^{\mathrm{e}}_{\mathrm{GNSS}} - \hat{p}^{\mathrm{e}}) + K_{pv}(v^{\mathrm{e}}_{\mathrm{GNSS}} - C_v\hat{v}^{\mathrm{e}}),\\
\dot{\hat{v}}^{\mathrm{e}} &= -2S(\omega^{\mathrm{e}}_{\mathrm{ie}})\hat{v}^{\mathrm{e}} + \hat{f}^{\mathrm{e}} + g^{\mathrm{e}}(\hat{p}^{\mathrm{e}})\\
&\quad + \theta^2 K_{vp}(p^{\mathrm{e}}_{\mathrm{GNSS}} - \hat{p}^{\mathrm{e}}) + \theta K_{vv}(v^{\mathrm{e}}_{\mathrm{GNSS}} - C_v\hat{v}^{\mathrm{e}}),\\
\dot{\xi} &= -R(\hat{q}^{\mathrm{e}}_{\mathrm{b}})S(\hat{\sigma})f^{\mathrm{b}}_{\mathrm{IMU}}\\
&\quad + \theta^3 K_{\xi p}(p^{\mathrm{e}}_{\mathrm{GNSS}} - \hat{p}^{\mathrm{e}}) + \theta^2 K_{\xi v}(v^{\mathrm{e}}_{\mathrm{GNSS}} - C_v\hat{v}^{\mathrm{e}}),\\
\hat{f}^{\mathrm{e}} &= R(\hat{q}^{\mathrm{e}}_{\mathrm{b}})f^{\mathrm{b}}_{\mathrm{IMU}} + \xi,
\end{aligned}
$$

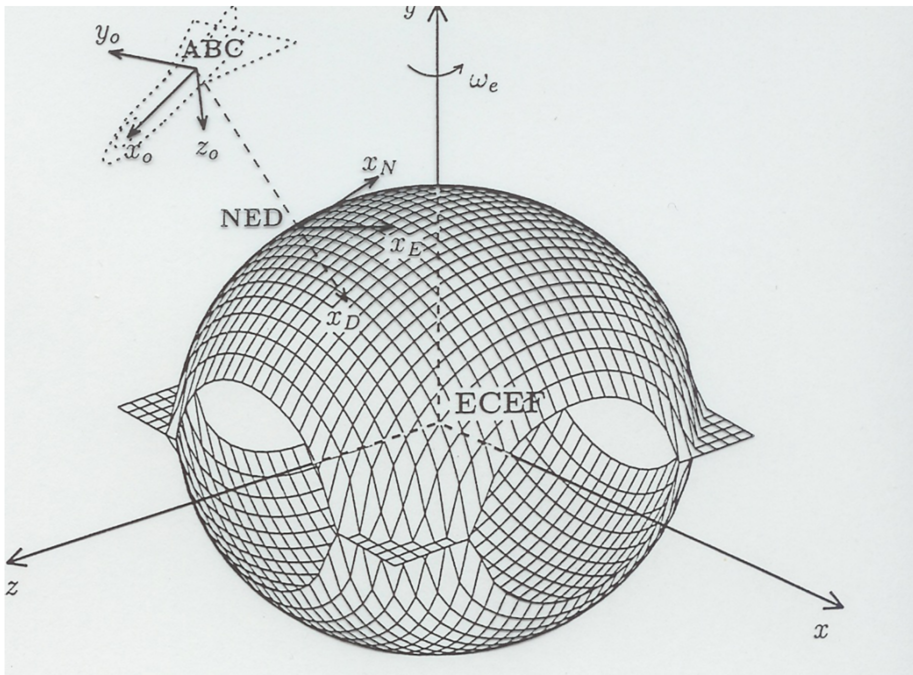

Attitude Observer

$$
\begin{aligned}
\dot{\hat{q}}^{\mathrm{e}}_{\mathrm{b}} &= \frac{1}{2}\hat{q}^{\mathrm{e}}_{\mathrm{b}} \otimes (\bar{\omega}^{\mathrm{b}}_{\mathrm{ib,IMU}} - \bar{\hat{b}}^{\mathrm{b}} + \bar{\hat{\sigma}}) - \frac{1}{2}\bar{\omega}^{\mathrm{e}}_{\mathrm{ie}} \otimes \hat{q}^{\mathrm{e}}_{\mathrm{b}}\\
\dot{\hat{b}}^{\mathrm{b}} &= \mathrm{Proj}(\hat{b}^{\mathrm{b}}, -k_I\hat{\sigma}),
\end{aligned}
$$

Nonlinear Injection Term

$$
\hat{\sigma} := k_1 m^{\mathrm{b}}_{\mathrm{IMU}} \times R(\hat{q}^{\mathrm{e}}_{\mathrm{b}})' m^{\mathrm{e}} + k_2 f^{\mathrm{b}}_{\mathrm{IMU}} \times R(\hat{q}^{\mathrm{e}}_{\mathrm{b}})' \,\mathrm{sat}_{M_f}(\hat{f}^{\mathrm{e}})
$$

Grip, H. F., T. I. Fossen, T. A. Johansen and A. Saberi. Globally Exponentially Stable Attitude and Gyro Bias Estimation with Application to GNSS/INS Integration. *Automatica*. Volume 51, January 2015, Pages 158–166.

Grip, H. F., T. I. Fossen, T. A. Johansen and A. Saberi. Nonlinear Observer for GNSS-Aided Inertial Navigation with Quaternion-Based Attitude Estimation. Proc. of ACC'13, Washington DC, 17-19 June.

NTNU

The eXogenous Kalman Filter (XKF)

The XKF is a nonlinear observer bridging the gap to the "*Kalman filter*" by:

- Improved filtering and optimality of noisy signals (performance improvement)
- Compute a covariance matrix (fault handling etc.)

Johansen, T. A. and T. I. Fossen. The eXogenous Kalman Filter (XKF).
International Journal of Control, Vol. 90 , Issue 2, 2017. pp. 161-167.

The Extended Kalman Filter (EKF)

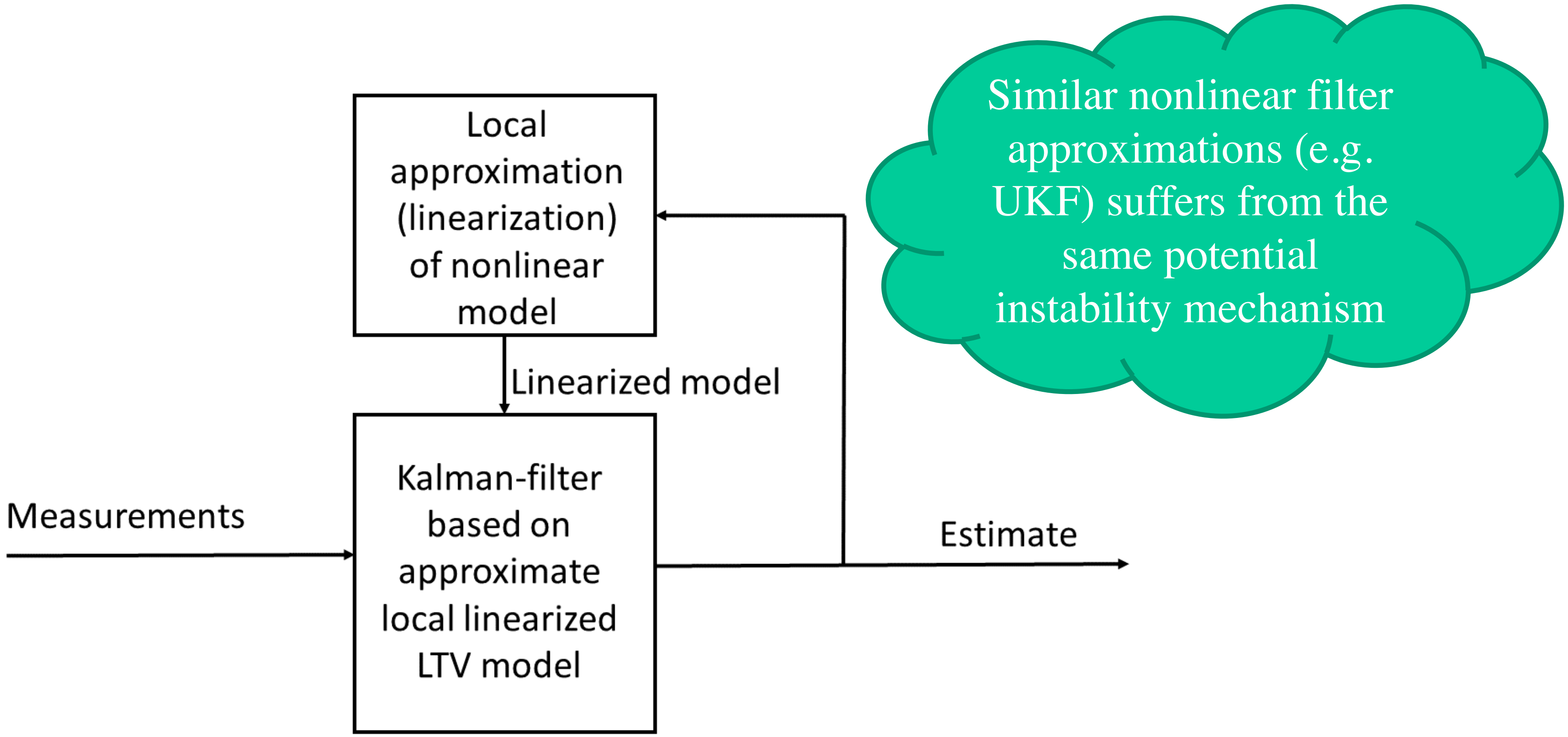

*Using the state estimate for linearization creates a **feedback loop** that can **destabilize the EKF** if the state estimate is not sufficiently accurate.*

The eXogenous Kalman Filter (XKF)

- The time-varying Kalman Filter (KF) is GES and optimal in the sense of minimum variance under some conditions.
- Nonlinear approximations such as the EKF linearizes the system about the estimated state trajectories, leading in general to loss of both global stability and optimality.
- Nonlinear observers tend to have strong, often global, stability properties. They are, however, often designed without optimality objectives considering the presence of unknown measurement errors and process disturbances.

- The XKF is a two-stage estimator combining a global nonlinear observer with a linearized KF in cascade. The estimate from the nonlinear observer is an exogenous signal only used for generating a linearized model to the KF. The XKF inherits the global stability property of the nonlinear observer, and simulations indicate that local optimality properties similar to a perfectly linearized KF can be achieved.

Johansen, T. A. and T. I. Fossen. The eXogenous Kalman Filter (XKF). *International Journal of Control*, Vol. 90 , Issue 2, 2017. pp. 161-167.

The eXogenous Kalman Filter (XKF)

This involves a **linearized KF** but not an EKF:
There is no feedback loop that can cause instability!

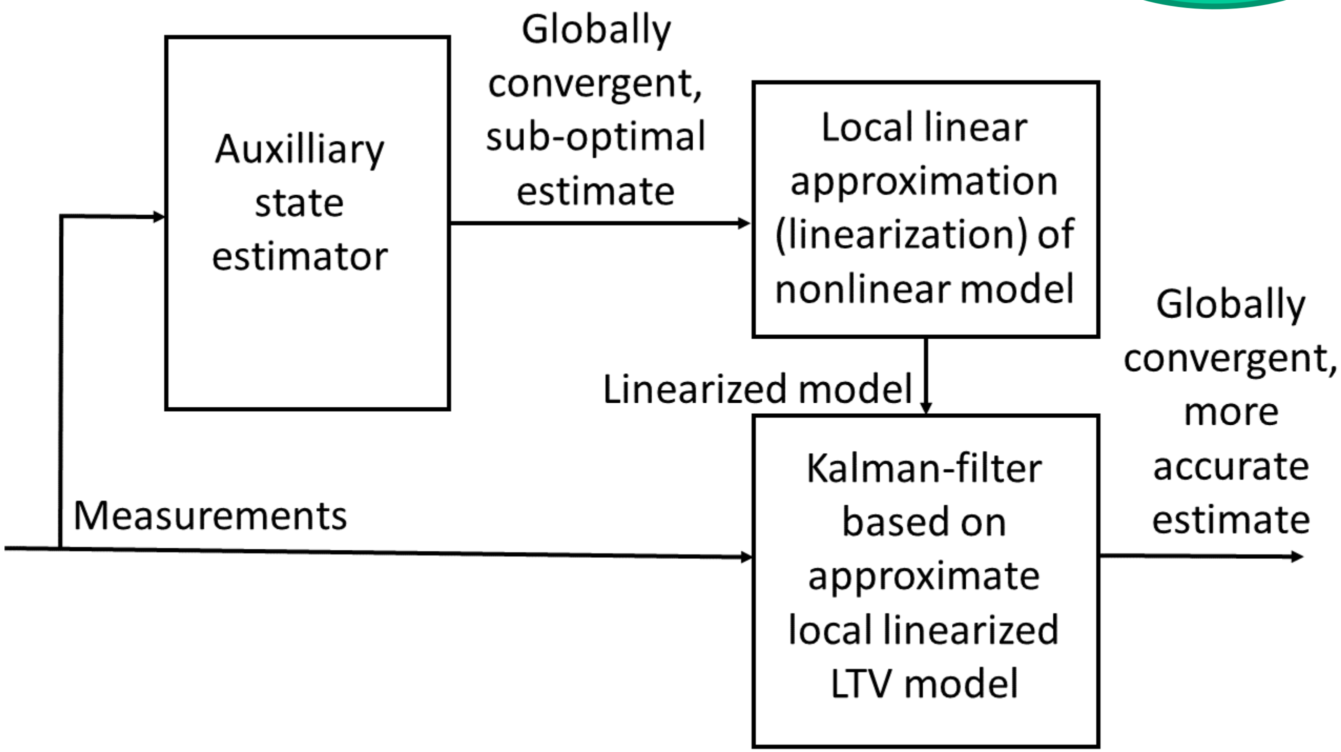

Main Result

The XKF inherits the nominal stability properties of the auxilliary state estimator (e.g. Nonlinear Observer) since it is a cascade structure.

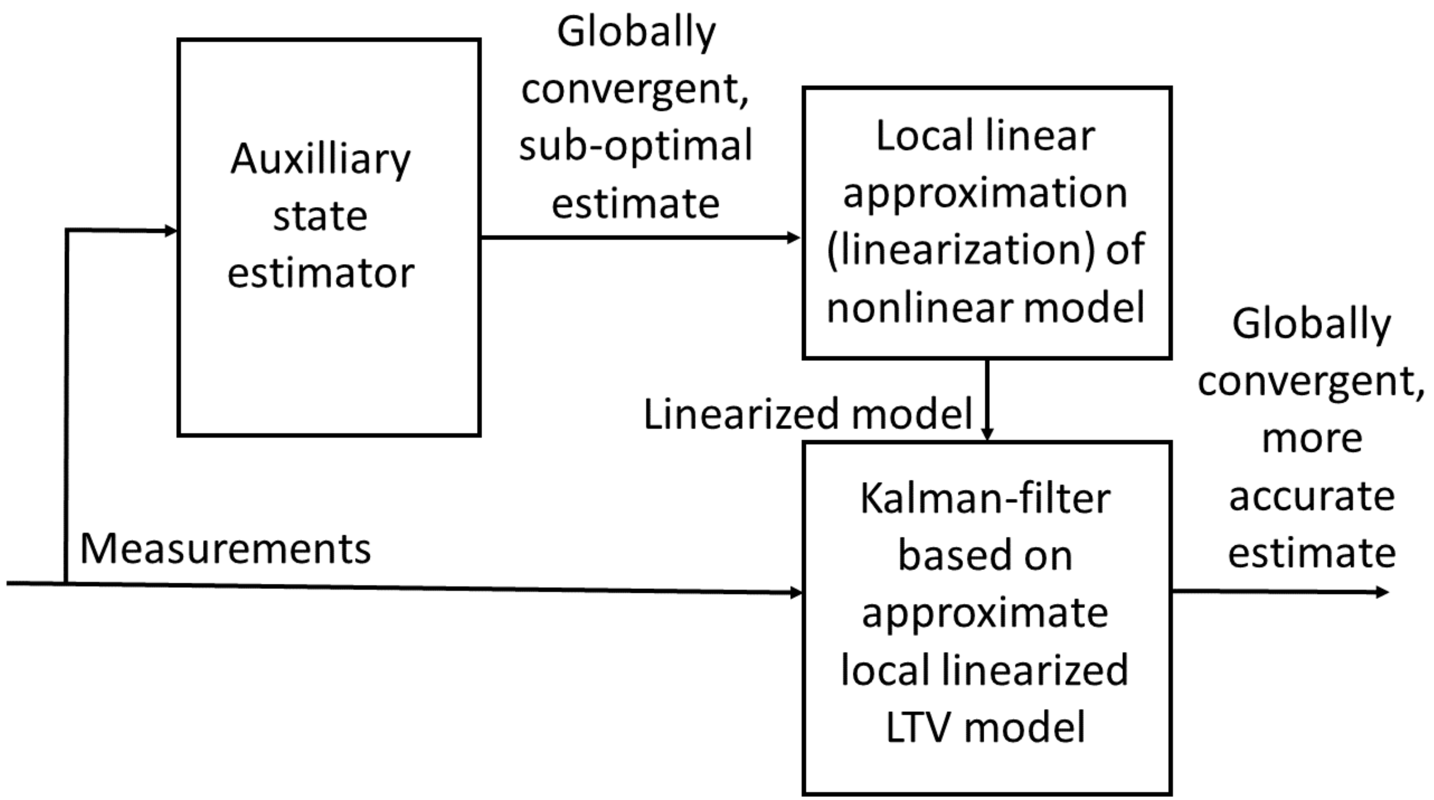

Johansen, T. A. and T. I. Fossen. The eXogenous Kalman Filter (XKF). *International Journal of Control*, Vol. 90 , Issue 2, 2017. pp. 161-167.

Analysis of Stability

$$\dot{x}(t) = f(x(t),t) + G(t)w(t) \quad (1)$$
$$y(t) = h(x(t),t) + e(t) \quad (2)$$

Linearization point given by the 1st-stage auxilliary state estimator

$\bar{x}$ is the exogenous signal from a nonlinear observer

$\breve{x}(t) = x(t) - \bar{x}(t)$ is the error dynamics

A Taylor series expansion of (1) about the trajectory $\bar{x}(t)$ gives

$$\begin{aligned}\dot{x}(t) &= f(\bar{x}(t),t) + F(\bar{x}(t),t)\breve{x}(t) \\ &\quad + G(t)w(t) + q(x(t),\bar{x}(t),t) \qquad (3)\\ y(t) &= h(\bar{x}(t),t) + H(\bar{x}(t),t)\breve{x}(t) \\ &\quad + r(x(t),\bar{x}(t),t) + e(t) \qquad (4)\end{aligned}$$

where $q(\cdot)$ and $r(\cdot)$ are higher-order terms, and

$$F(\bar{x},t) := \frac{\partial f}{\partial x}(\bar{x},t), \qquad H(\bar{x},t) := \frac{\partial h}{\partial x}(\bar{x},t)$$

$$||q(t)|| \leq k_q||\breve{x}(t)||^2, \ \ ||r(t)|| \leq k_r||\breve{x}(t)||^2$$

Linearized Kalman Filter

Use the truncated (linearized) model for design of a standard LTV Kalman Filter:

$$\begin{aligned}\dot{\hat{x}}(t) &= f(\bar{x}(t),t) + F(\bar{x},t)(\hat{x}(t) - \bar{x}(t)) \\ &\quad + K(t)\left(y(t) - h(\bar{x}(t),t) - H(\bar{x}(t),t)(\hat{x} - \bar{x}(t))\right)\end{aligned} \tag{6}$$

$$K(t) = P(t)H^T(\bar{x}(t),t)R^{-1}$$

$$\begin{aligned}\dot{P}(t) &= F(\bar{x}(t),t)P(t) + P(t)F^T(\bar{x}(t),t) \\ &\quad + G(t)QG^T(t) - K(t)RK^T(t)\end{aligned} \tag{7}$$

Theorem 1: Suppose there are no noises, i.e. $w = 0$ and $e = 0$, and assume

A1. The LTV system $(F(\bar{x}(t),t), G(t), H(\bar{x}(t),t))$ is uniformly completely observable and controllable.

A2. The nominal error dynamics Σ_2 of the auxiliary state estimator is Uniformly Globally Asymptotically Stable (UGAS), Semi-Globally Exponentially Stable (SGES), or Globally Exponentially Stable (GES).

A3. The LKF tuning parameters $P(0), Q, R$ are symmetric and positive definite.

Then the origin $\check{x} = \tilde{x} = 0$ of the nominal error dynamics cascade $\Sigma_2 - \Sigma_1$ (see Figure 2) inherits the stability properties of Σ_2.

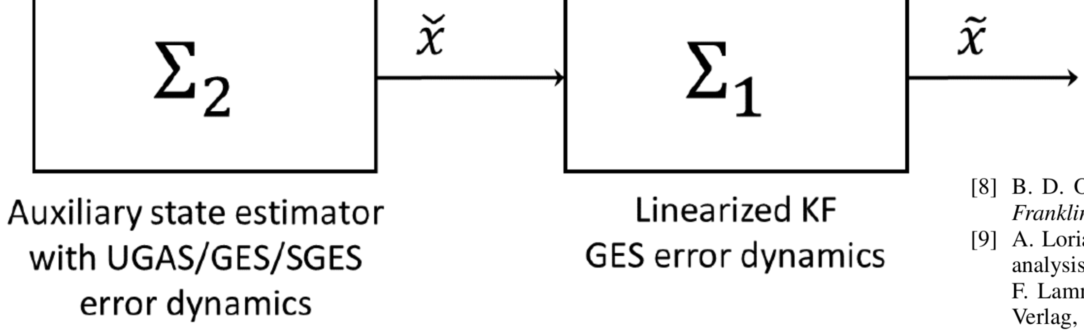

Fig. 2. Cascaded nominal error dynamics (no noise).

[8] B. D. O. Anderson, "Stability properties of Kalman-Bucy filters," *J. Franklin Institute*, vol. 291, pp. 137–144, 1971.

[9] A. Loria and E. Panteley, "Cascaded nonlinear time-varying systems: analysis and design," in *Advanced Topics in Control Systems Theory*, F. Lamnabhi-Lagarrigue, A. Loria, and E. Panteley, Eds. Springer-Verlag, London, 2004, ch. 2.

Example 1

First-order linear dynamics with nonlinear measurement functions

$$\dot{x} = u$$

$$y_1 = |x - 1|$$

$$y_2 = |x + 2|$$

A nonlinear observer can be designed for this system using the following nonlinear transform of the measurements

$$\begin{aligned} z &= y_2^2 - y_1^2 && (11)\\ &= x^2 + 4x + 4 - \left(x^2 - 2x + 1\right) && (12)\\ &= 6x + 3 && (13) \end{aligned}$$

which leads to the nonlinear observer

$$\dot{\bar{x}} = u + L\left(y_2^2 - y_1^2 - 6\bar{x} - 3\right) \quad (14)$$

with error dynamics $\breve{x} = x - \bar{x}$ given by the linear system

$$\Sigma_2 : \ \dot{\breve{x}} = -6L\breve{x} \quad (15)$$

Clearly, Σ_2 is GES for any constant $L > 0$ which should be chosen to achieve desired filtering bandwidth or pole locations. For completeness, the discrete-time implementation is given by the Euler discretization method

$$\bar{x}(k+1) = \bar{x}(k) + Tu(k) + TL\left(y_2^2(k) - y_1^2(k) - 6\bar{x}(k) - 3\right) \quad (16)$$

LKF∗ is a perfect LKF linearized about the true (unknown) trajectory (perfect reference signal).

The control input u is a unit square wave signal with period 2π.

The EKF does not converge while all other estimators converge due to their GES property.

In particular LKF∗ has a very accurate initial linearization that is exploited to make an accurate correction already at time $k = 0$.

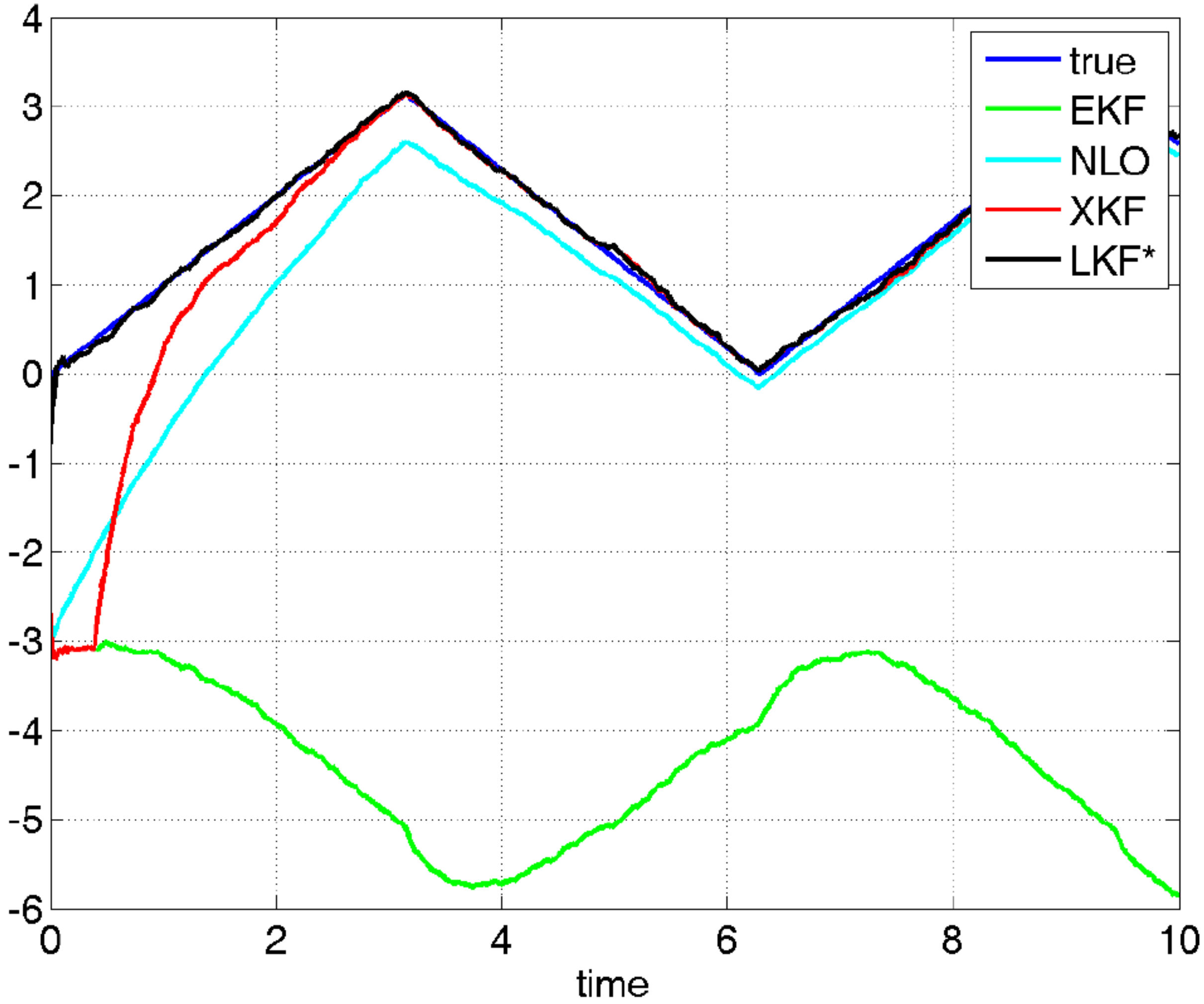

Figure 3. Simulation results, first example.

Example 2

First-order nonlinear dynamics with linear measurement function:

$$\dot{x} = -2x + x|x| + u$$
$$y = x$$

We note that this system is only locally stable. For this system an NLO can be desiged as

$$\dot{\bar{x}} = -2\bar{x} + \bar{x}|y| + u + L(y - \bar{x}) \tag{23}$$

The error dynamics $\breve{x} = x - \bar{x}$ is given by the system

$$\Sigma_2 : \; \dot{\breve{x}} = (-2 + |y| - L)\breve{x} \tag{24}$$

Choosing $L = |y| + L_0$ leads to $\dot{\bar{x}} = -(2 + L_0)\bar{x}$ which is GES for any constant $L_0 > -2$ which should be chosen to achieve desired filtering performance. Discretization and design of EKF and XKF are similar to the previous example.

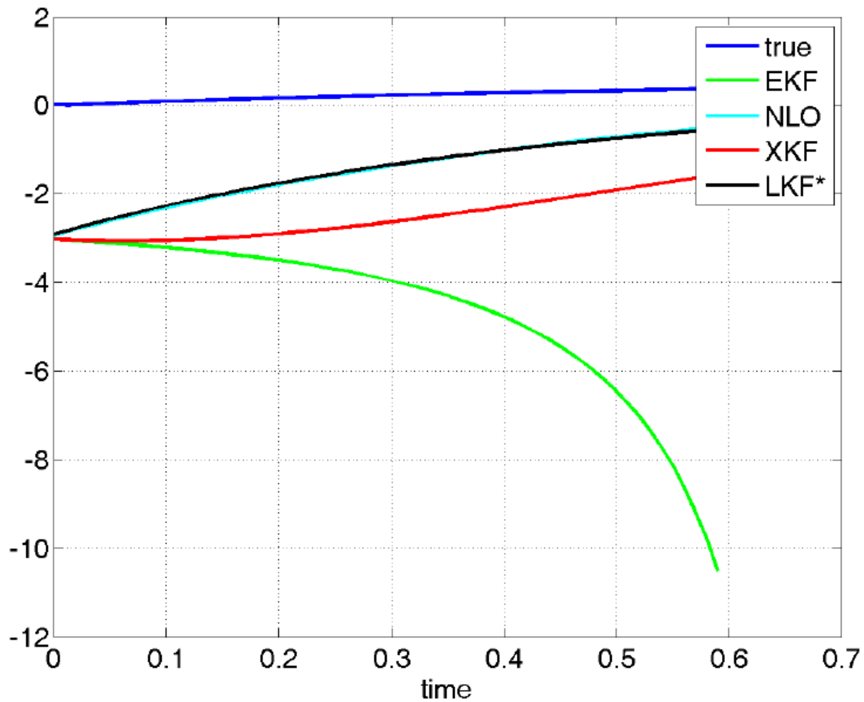

(a) Initial condition $\hat{x}(0) = \eta(0) = -3$.

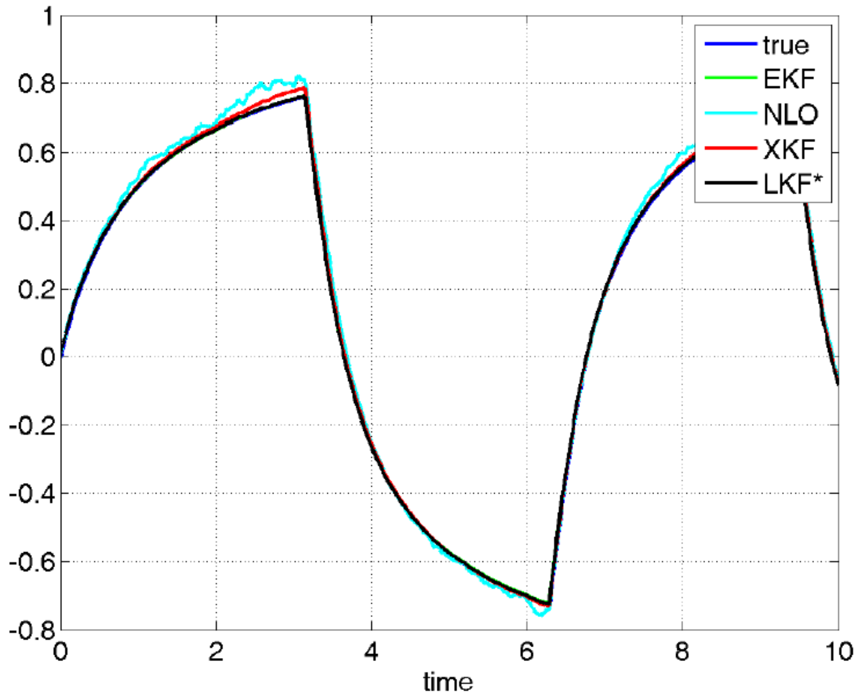

(b) Initial condition $\hat{x}(0) = \eta(0) = 0$.

Figure 4. Simulation results, second example. Note that the curves of the NLO and LKF* are almost indistinguishable in (a), while in (b) is curves of the EKF, XKF and LKF* are almost indistinguishable from the true state. (a) Initial condition $\hat{x}(0) = \eta(0) = -3$. (b) Initial condition $\hat{x}(0) = \eta(0) = 0$.

Low-Cost Integrated Navigation Systems - Applications

- Unmanned Aerial Vehicles (UAVs)
- Surface Ships
- Autonomous Underwater Vehicles (AUVs)

Fleet of the NTNU Unmanned Aerial Laboratory (UAV-Lab)

Procurement and operation license from Norwegian CAA (Civil Aviation Authority) for VLOS/BLOS operations since 2014

- Penguin B fixed-wing (VLOS/EVLOS/BLOS)
- 3D Robotics hexa-copters (VLOS)
- Microdrone quadro-copter (VLOS)
- X8 fixed-wing (VLOS)

NTNU Airfield at Agdenes

Located 94 km North-West of Trondheim

We also use the airports at Eggemoen and Ørland

Unmanned Aerial Vehicle (UAVs)

Strapdown INS aided by:

- GNSS measurements
- Time-delayed GNSS measurements
- GNSS and camera measurements (optical flow)

Estimation of wind: angle-of-attack and sideslip angle

Penguin B

X8 Skywalker

Nonlinear Observers for INS aided by GNSS

Development of low-cost integrated strapdown navigation systems (nonlinear observers) using inertial and pseudo-range/carrier-phase measurements.

- Nonlinear observers for tight integration of INS aided by GNSSS
- Nonlinear observers for GNSS time-delayed aided INS
- Nonlinear observers for aided INS using pseudo-range and carrier-phase measurements (RTK)

T. A. Johansen, T. I. Fossen and J. M. Hansen (2017).
Nonlinear Observer for Tightly Integrated Inertial Navigation Aided by Pseudo-Range Measurements.
Journal of Dynamic Systems, Measurement and Control,
Vol. 139(1), January 2017.

J. M. Hansen, T. I. Fossen and T. A. Johansen (2017).
Nonlinear Observer Design for GNSS-Aided Inertial Navigation Systems with Time-Delayed GNSS Measurements.
Control Engineering Practice, Vol. 60, March 2017, pp. 39–50.

Validation of INS/GNSS Nonlinear Observer against EKF

EKF: Extended Kalman filter implementation

NLO-Mag: magnetometer is used as attitude reference vector

NLO-Vel: assumes that heading and course to coincide (avoid compass) when computing the velocity reference vectors

Table 3. Observer performance comparison (NED position in m, attitude in deg and speed in m/s)

		EKF			NLO-Mag			NLO-Vel		
Dataset 1	POS RMS:	3.43	2.71	2.62	3.37	2.62	2.50	3.37	2.63	2.50
	POS STD:	2.60	2.44	2.46	2.48	2.41	2.44	2.48	2.42	2.44
	ATT RMS:	1.83	2.59	5.50	2.02	2.69	5.46	1.93	3.01	6.88
	ATT STD:	1.67	1.81	5.42	1.84	1.90	5.28	1.90	1.92	6.15
	SPE RMS:		0.60			0.67			0.69	
	SPE STD:		0.59			0.66			0.69	
Dataset 2	POS RMS:	4.43	4.40	3.43	3.38	5.00	3.63	3.37	5.00	3.63
	POS STD:	2.53	4.35	2.86	2.46	4.20	2.82	2.46	4.20	2.82
	ATT RMS:	1.76	1.87	6.39	2.09	1.87	7.85	1.56	1.94	6.36
	ATT STD:	1.70	1.66	6.34	1.73	1.67	6.28	1.46	1.59	6.36
	SPE RMS:		0.86			1.06			1.05	
	SPE STD:		0.83			1.02			1.02	

Hansen, J. M., J. Rohác, M. Šipoš, T. A. Johansen and T. I. Fossen (2016). Validation and Experimental Testing of Observers for Robust GNSS-Aided Inertial Navigation. In "Recent Advances in Robotic Systems. (G. Wang, Ed.), InTech, Vienna. <Open Access: http://intechweb.org/>. ISBN 978-953-51-4767-1

Validation of INS/GNSS Nonlinear Observer against EKF

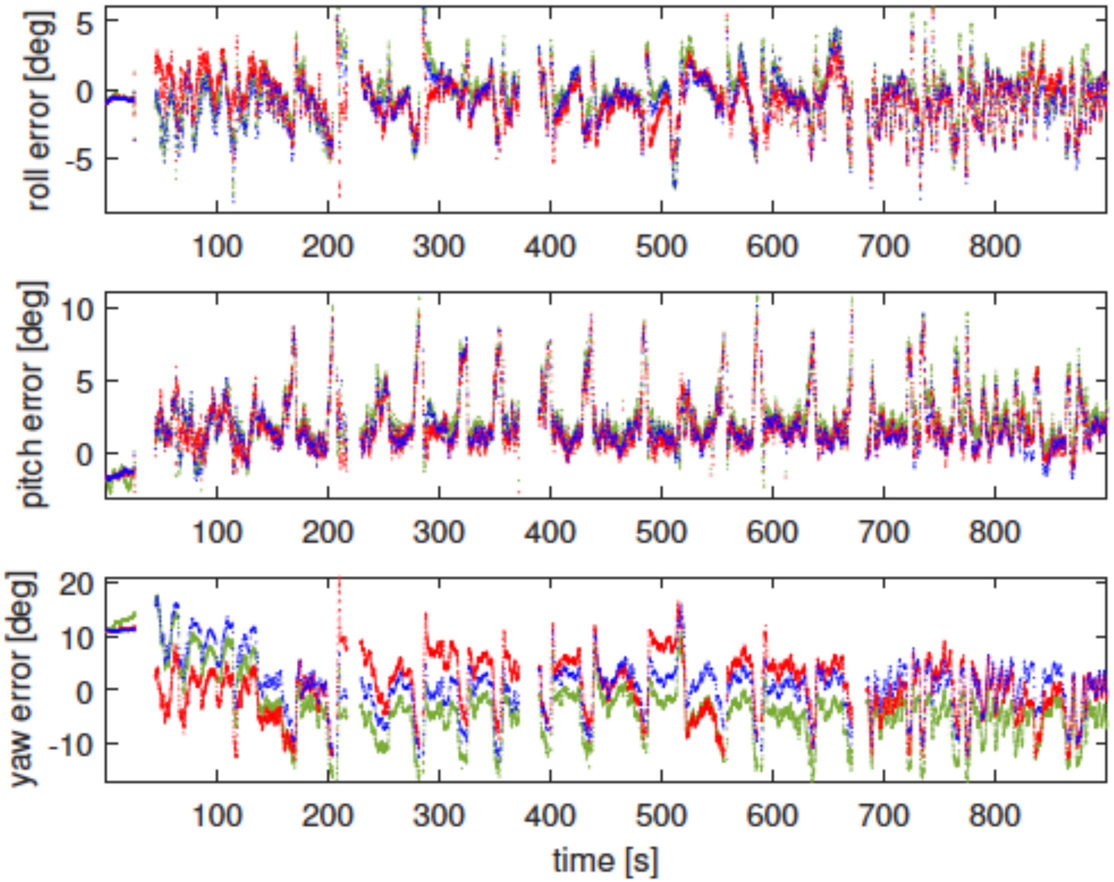

Figure 15. Attitude error (Dataset 1): EKF (red), NLO-Mag (blue dashed), NLO-Vel (green)

Figure 16. Position estimation error (Dataset 1): EKF (red), NLO-Mag (blue dashed), NLO-Vel (green)

Hansen, J. M., J. Rohác, M. Šipoš, T. A. Johansen and T. I. Fossen (2016). Validation and Experimental Testing of Observers for Robust GNSS-Aided Inertial Navigation. In "Recent Advances in Robotic Systems. (G. Wang, Ed.), InTech, Vienna. <Open Access: http://intechweb.org/>. ISBN 978-953-51-4767-1

Validation of INS/GNSS Nonlinear Observer against EKF

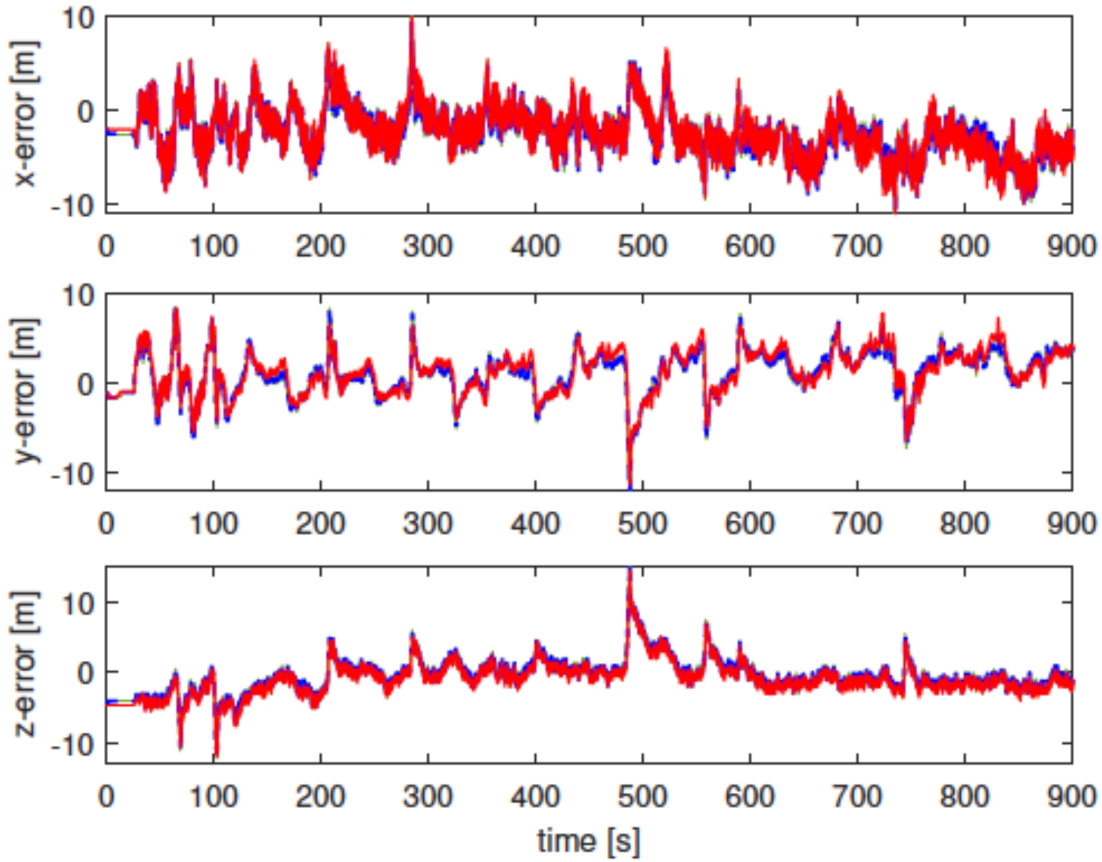

Figure 16. Position estimation error (Dataset 1): EKF (red), NLO-Mag (blue dashed), NLO-Vel (green)

Hansen, J. M., J. Rohác, M. Šipoš, T. A. Johansen and T. I. Fossen (2016). Validation and Experimental Testing of Observers for Robust GNSS-Aided Inertial Navigation. In "Recent Advances in Robotic Systems. (G. Wang, Ed.), InTech, Vienna. <Open Access: http://intechweb.org/>. ISBN 978-953-51-4767-1

Nonlinear Observers for INS aided by GNSS

GNSS time-delay: Where?

There is a delay arising at the GNSS-receiver due to computational time and an internal transport delay. The delay is defined as the time from input to output of the receiver.

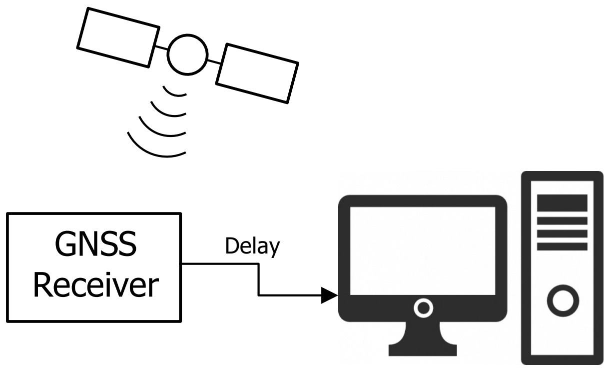

Time-delay: Determination

The GNSS-receiver has a Pulse-Per-Second (PPS) signal timed (rising edge) with GPS time. The time-delay is measured as the time between the PPS signal and the end of a data package. The data frequency is 1-10 Hz leaving multiple packages per PPS signal.

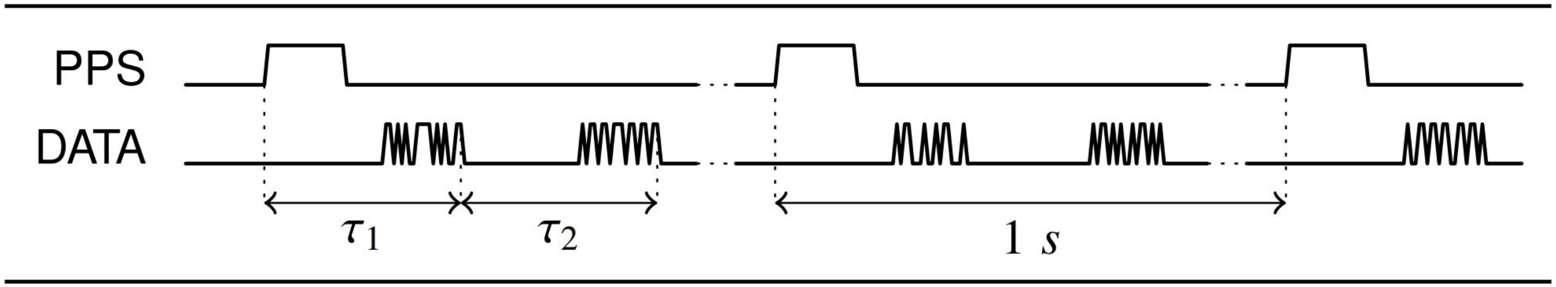

Hansen, J. M., T. I. Fossen and T. A. Johansen (2017). Nonlinear Observer Design for GNSS-Aided Inertial Navigation Systems with Time-Delayed GNSS Measurements. *Control Engineering Practice*, Vol. 60, March 2017, Pages 39–50.

Nonlinear Observers for INS aided by GNSS – Time-Delay Modification

The observer is being altered to take the time-delay into account by adapting the acceleration delayed approach, and delaying the IMU and magnetometer data.

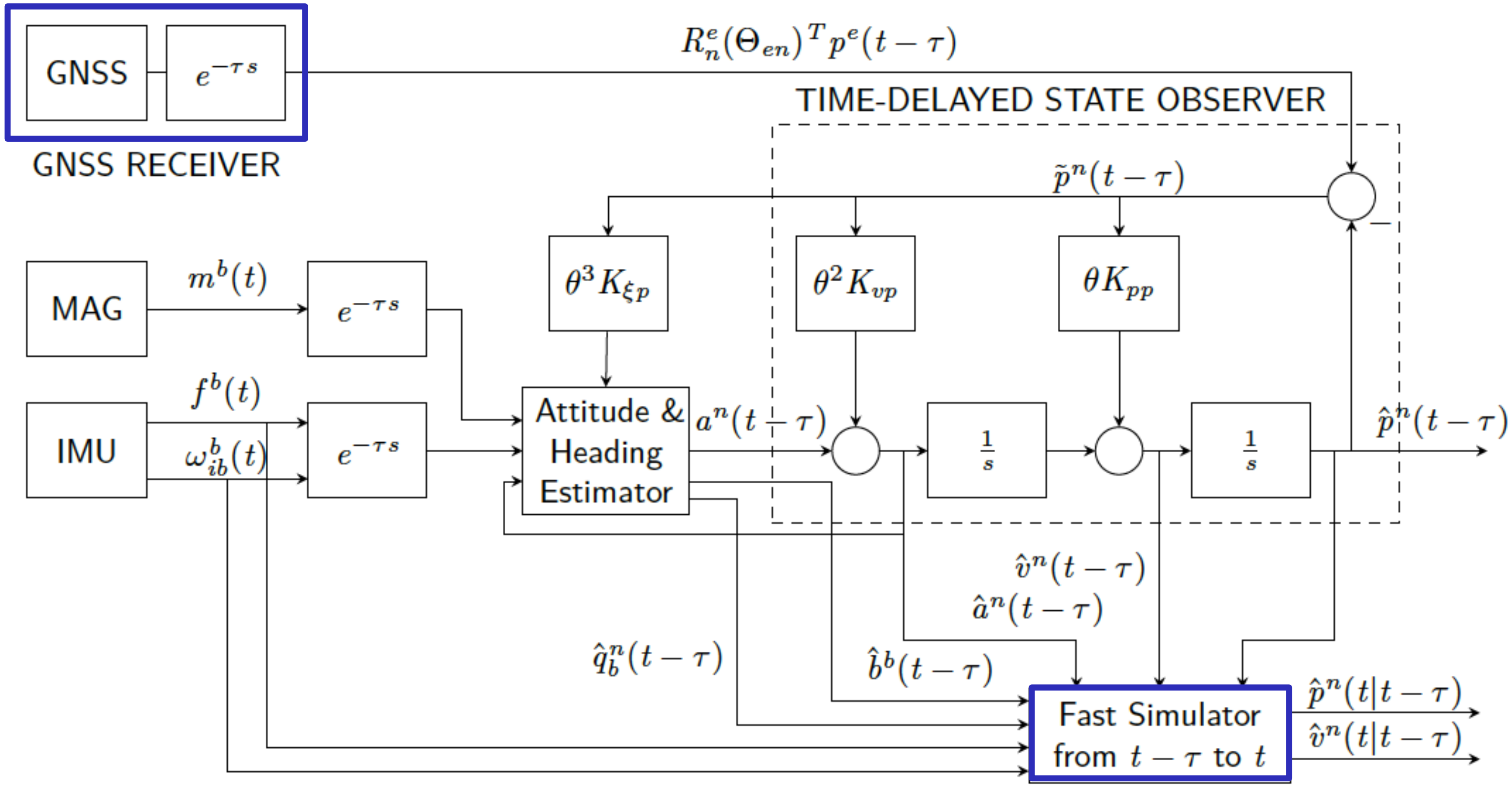

A fast simulator (predictor) is used to predict the current position and velocity.

NTNU UAV equipped with INS for Data logging

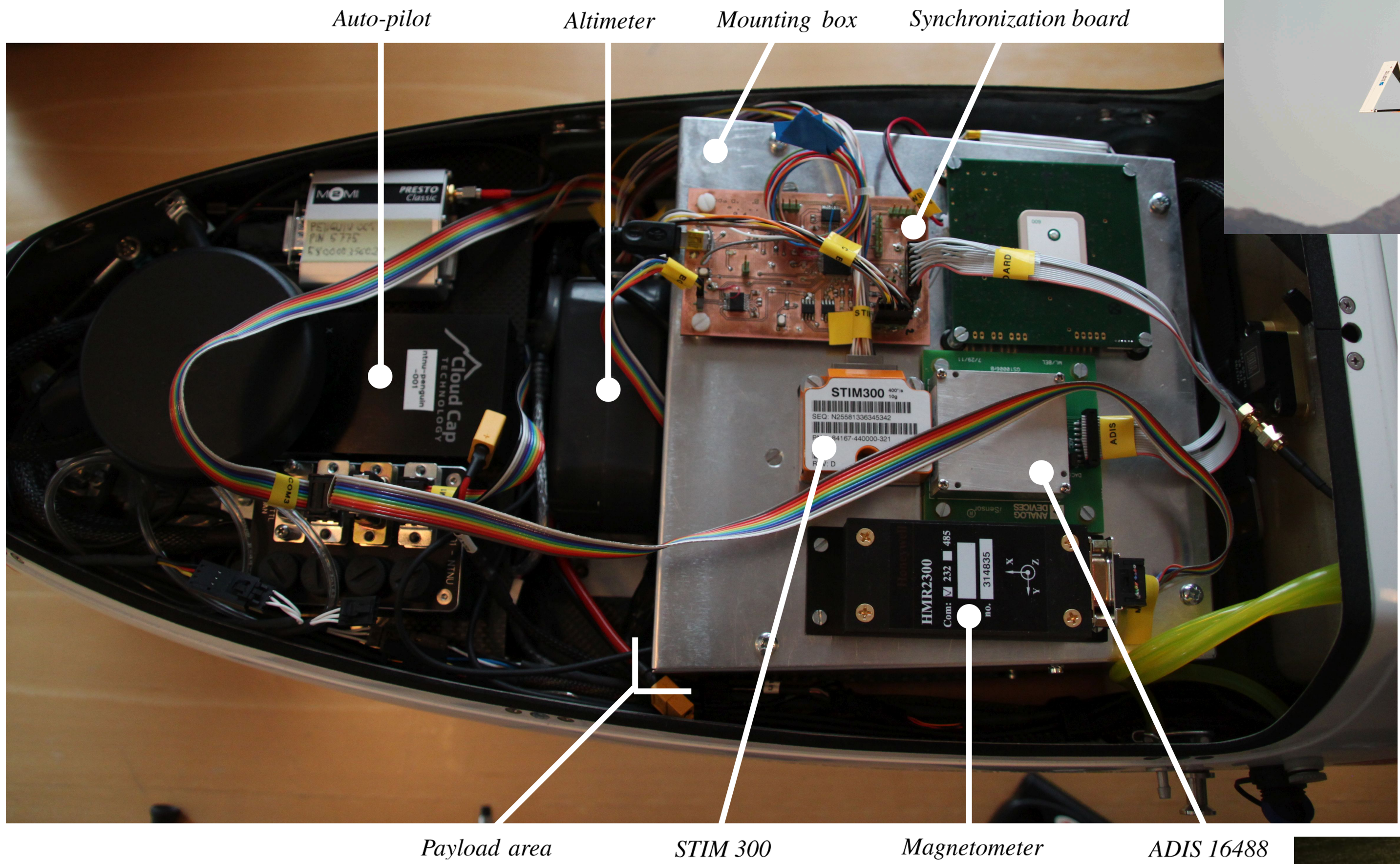

Penguin navigation payload: Two IMUs, optical camera, infrared camera, RTK GPS and embedded controller for data logging

Nonlinear Observers for INS aided by GNSS – Time-Delay Modification

Time-Delay: Experimental Results

The GNSS-receiver time delay is approx. 154 ms, which for the Penguin UAV at max speed results in a position error of 5.5 m.

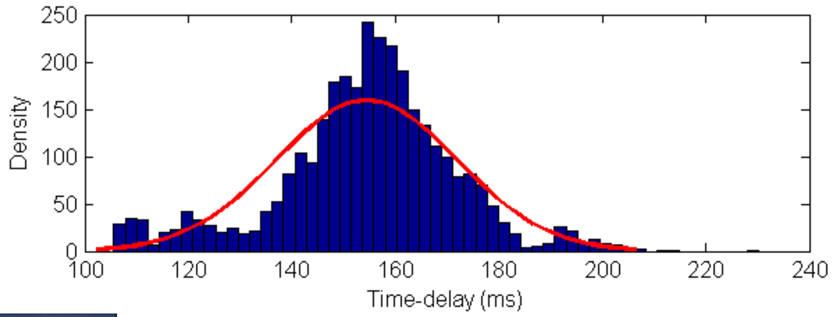

Hansen, J. M., T. I. Fossen and T. A. Johansen (2015). Nonlinear Observer for INS Aided by Time-Delayed GNSS Measurements - Implementation and UAV Experiments. *Proc. of the 2015 International Conference on Unmanned Aircraft Systems* (ICUAS'15), Denver, Colorado.

Hansen, J. M., T. I. Fossen and T. A. Johansen (2017). Nonlinear Observer Design for GNSS-Aided Inertial Navigation Systems with Time-Delayed GNSS Measurements. Control Engineering Practice, Vol. 60, March 2017, Pages 39–50.

Nonlinear Observers for INS aided by GNSS – Time-Delay Modification

Experiments were carried out at Eggemoen airport in 2014/2015.

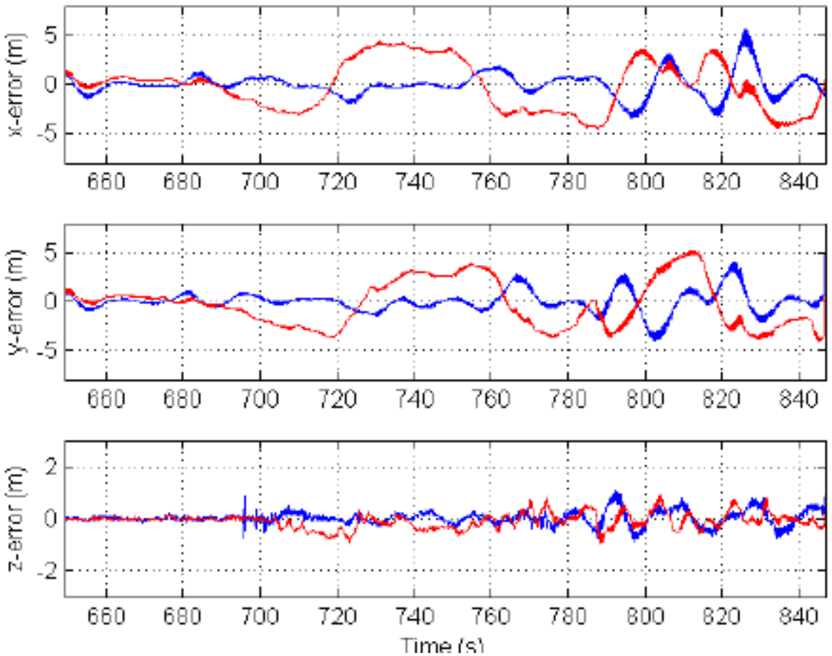

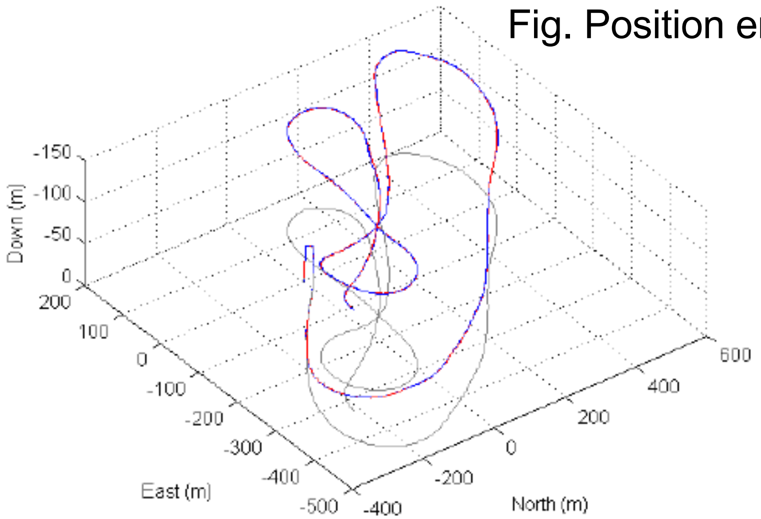

Fig. Position errors.

Fig. GPS in Google Earth

The Skywalker X8 with Pixhawk Autopilot

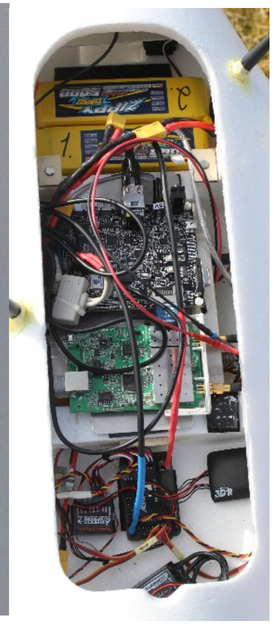

- 18 m/s cruise speed
- Catapult launch
- Belly or net landing
- Electric, <1 hr endurance
- Large payload bay
- >1 kg payload capacity
- Inexpensive
- Flexible avionics and payload system integration with Pixkhawk open source autopilot
- Currently telemetry on 433 MHz or 5.8 GHz radio for VLOS
- Can be set up for BLOS with GPRS and VHF radio links

Autonomous Launch and Recovery Systems for Maritime and Offshore Operations

First Attempt: Automatic Net Landing in 2015

R. Skulstad, C. K. Syversen, M. Merz, N. Sokolova, T. I. Fossen, T. A. Johansen, Autonomous Net Recovery of Fixed-Wing UAV with Single-Frequency Carrier-Phase Differential GNSS, *IEEE Aerospace and Electronic Systems Magazine*, 2015

Automatic Net Landing onboard a Research Vessel outside the Azores in Portugal in 2016

Safety-Critical Offshore Operations

- Accurate landing on ships and offshore structures with fixed-wing UAVs is a safety-critical operations since the aircraft can hit an object with causes fire/explosions even if the best technology is used.
- An obvious solution is to land the fixed-wing UAV in a safe distance from the ship and catch the UAV with a second UAV. Boeing and NTNU have one approach each:

- **Insitu FLARES (Boeing owns Insitu and the IPR)**
- **NTNU AMOS fixed-wing net-recovery approach (Patent filed April 12, 2017)**

Kristian Klausen (PhD defense is scheduled for 23 June 2017)
"Coordinated Control of Multirotors for Suspended Load Transportation and Fixed-Wing Net Recovery".
Supervisors: *Professors Thor I. Fossen and Tor Arne Johansen,* NTNU

K. Klausen, J. B. Moe, J. C. van den Hoorn, A. Gomola, T. I. Fossen and T. A. Johansen (2016), Coordinated Control Concept for Recovery of a Fixed-Wing UAV on a Ship using a Net Carried by Multirotor UAVs, ICUAS'16, Arlington, USA

Insitu FLARES

Since 2014 Insitu has developed the Flying Launch and Recovery System (FLARES), a system designed to launch and recover the ScanEagle without the need to transport and assemble the launch catapult and recovery crane.

It consists of second, quadrotor UAV that carries the ScanEagle vertically and releases it into forward flight. For recovery, the quadrotor hovers trailing a cable that it captures, as it would the cable from the SkyHook crane.

The ScanEagle fixed-wing UAV

The NTNU AMOS Ship-Landing Concept

Cooperative Control: A suspended net is transported away from the ship to a safe distance by using two or more multicopters, which cooperates. They UAVSs are intelligent and share positions in order to control the tension of the net.

Coordinated Control: Master-Slave Principle:
The fixed-wing aircraft acts like an master, while the cooperative multicopters is the slave following the master.

Virtually-Moving Airfield: The airfield/net is moved in an optimal manner vertically and horizontally to improve landing accuracy and reduce impact speed.

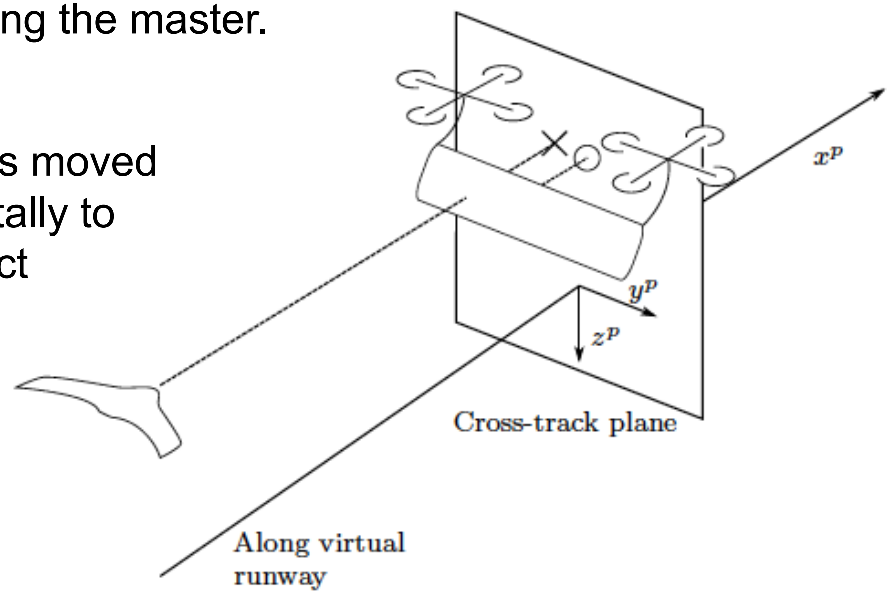

K. Klausen, J. B. Moe, J. C. van den Hoorn, A. Gomola, T. I. Fossen and T. A. Johansen. Coordinated Control Concept for Recovery of a Fixed-Wing UAV on a Ship using a Net Carried by Multirotor UAVs. *Proc. of the 2016 International Conference on Unmanned Aircraft Systems* (ICUAS'16), Arlington, VA, 7-10 June, 2016.

Robust UAV Attitude and Navigation System using Nonlinear Observers and Camera Measurements

PhD Candidate: Lorenzo Fusini

Sensor fusion of low-cost inertial sensors, magnetometers, sensors for altitude/depth/speed, GNSS and cameras using nonlinear observer theory.

- Classification of problems for robust navigation and autonomy
- Design a fault-tolerant robust navigation system for UAVs

NTNU

Pinhole Camera Model (M-Matrix)

Mapping from Optical Flow (OF) to BODY velocities

$$\begin{bmatrix} v^b_{b/n} \\ \omega^b_{b/n} \end{bmatrix} = -\underbrace{\begin{bmatrix} M_1(f, p^c_1) \\ \vdots \\ M_N(f, p^c_N) \end{bmatrix}^+}_{M+} \begin{bmatrix} \dot{r_1} \\ \dot{s_1} \\ \vdots \\ \dot{r_N} \\ \dot{s_N} \end{bmatrix}$$

Depends on the roll angle φ and pitch angle θ as well as attitude $c_z^h = -h$.

$$M_k(f, p^c_k) = \frac{f}{z^c_k} \begin{bmatrix} 0 & 1 & -\frac{y^c_k}{z^c_k} & -\frac{y^c_k(y^c_k)}{z^c_k} - z^c_k & \frac{y^c_k x^c_k}{z^c_k} & x^c_k \\ -1 & 0 & \frac{x^c_k}{z^c_k} & \frac{x^c_k y^c_k}{z^c_k} & -\frac{x^c_k(x^c_k)}{z^c_k} - z^c_k & y^c_k \end{bmatrix}$$

$$p^c = \begin{bmatrix} x^c \\ y^c \\ z^c \end{bmatrix} = \frac{c^n_z - z^n}{s\sin(\theta) + \cos(\theta)(f\cos(\phi) + r\sin(\phi))} \begin{bmatrix} s \\ -r \\ -f \end{bmatrix}$$

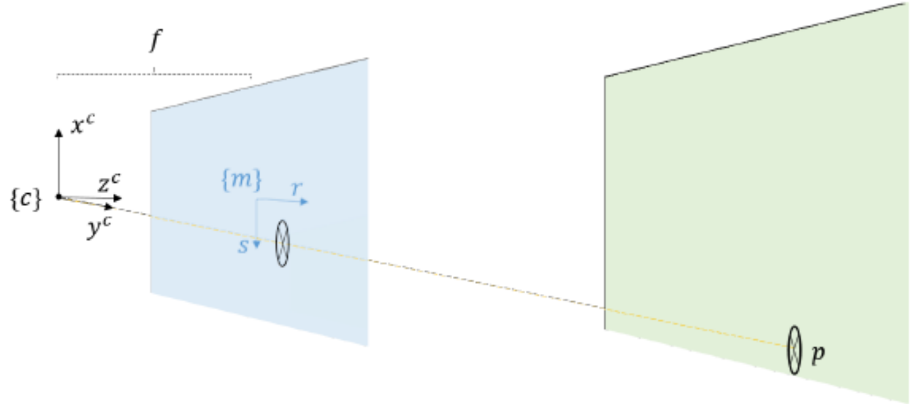

$$\frac{r}{f} = \frac{y^c}{z^c}$$

$$\frac{s}{f} = -\frac{x^c}{z^c}$$

Figure 3.1: The pinhole camera model maps a perceived point in the camera-fixed frame to the image plane.

Image Capturing (Optical Flow)

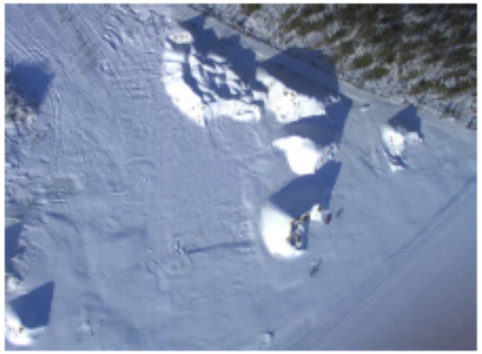

(a)

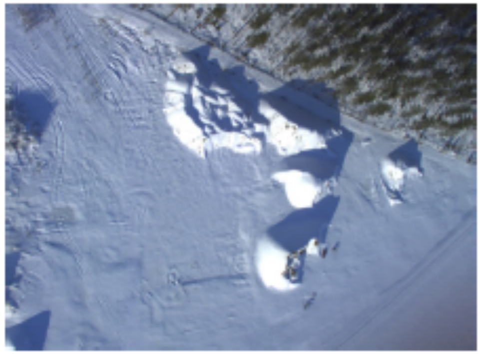

(b)

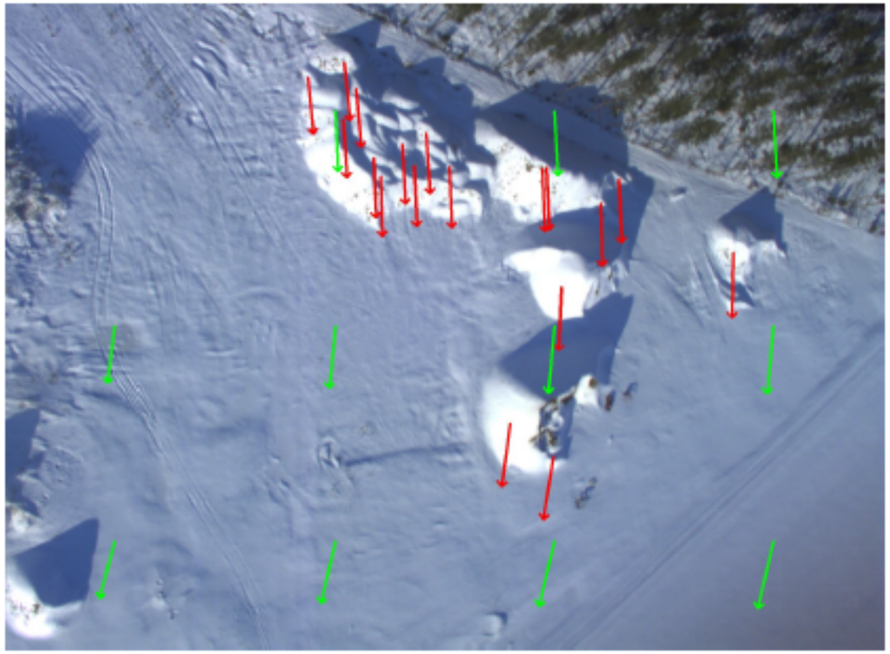

(c)

Fig. 2. a) Image captured at time t_0. b) Image captured at time $t_0 + \delta t$. c) Optical flow vectors between image a) and b), generated by SIFT (red) and Template Matching (green).

INS aided by Optical Flow: Ground Truth Optical Flow (GTOF) Observer

$$\Sigma_1 \begin{cases} \dot{\hat{R}} = \hat{R}S(\omega_m^b - \hat{b}^b) + \sigma K_P \hat{J} \\ \dot{\hat{b}}^b = \mathrm{Proj}(\hat{b}^b, -k_I \mathrm{vex}(\mathbb{P}_a(\hat{R}_s^T K_P \hat{J}))) \end{cases}$$

$$\Sigma_2 \begin{cases} \dot{\hat{p}}^n = \hat{v}^n + K_{pp}(p^n - \hat{p}^n) + K_{pv}(v^n - \hat{v}^n) \\ \dot{\hat{v}}^n = \hat{a}^n + g^n + K_{vp}(p^n - \hat{p}^n) + K_{vv}(v^n - \hat{v}^n) \\ \dot{\xi} = -\sigma K_P \hat{J} a^b + K_{\xi p}(p^n - \hat{p}^n) + K_{\xi v}(v^n - \hat{v}^n) \\ \hat{a}^n = \hat{R} a^b + \xi \end{cases}$$

$$\mathrm{OF} \left\{ \begin{bmatrix} \hat{v}_F^b \\ \hat{\omega}_F^b \end{bmatrix} = \hat{M}^+ \begin{bmatrix} \dot{r} \\ \dot{s} \end{bmatrix} \right.$$

A GES nonlinear observer has been developed using optical flow as a reference vector together with magnetometer and acceleration in the attitude observer

$$\hat{J}(a^b, \hat{a}^n, v_F^b, \hat{v}^n, \hat{R}) := \hat{A}_n A_b^T - \hat{R} A_b A_b^T$$
$$A_b := [a^b,\ a^b \times v_F^b,\ a^b \times (a^b \times v_F^b)]$$
$$\hat{A}_n := [\hat{a}^n,\ \hat{a}^n \times \hat{v}^n,\ \hat{a}^n \times (\hat{a}^n \times \hat{v}^n)]$$

Optical flow is used to compute a body-fixed velocity reference vector

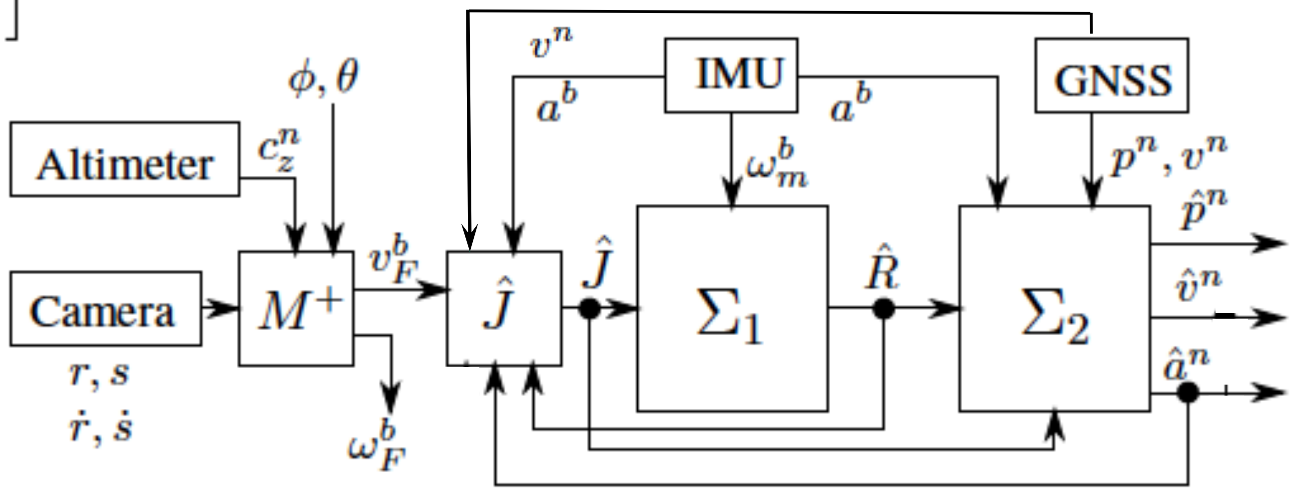

Fusini, L. T. I. Fossen and T. A. Johansen. Nonlinear Camera-Based INS for Fixed-Wing UAV using the eXogenous Kalman Filter. Ch. 2 in "Sensing and Control for Autonomous Vehicles: Applications to Land, Water and Air Vehicles" (T. I. Fossen, K. Y. Pettersen and H. Nijmeijer, Eds.). Springer, 2017.

Stability of GTOF Observer: Feedback Interconnection

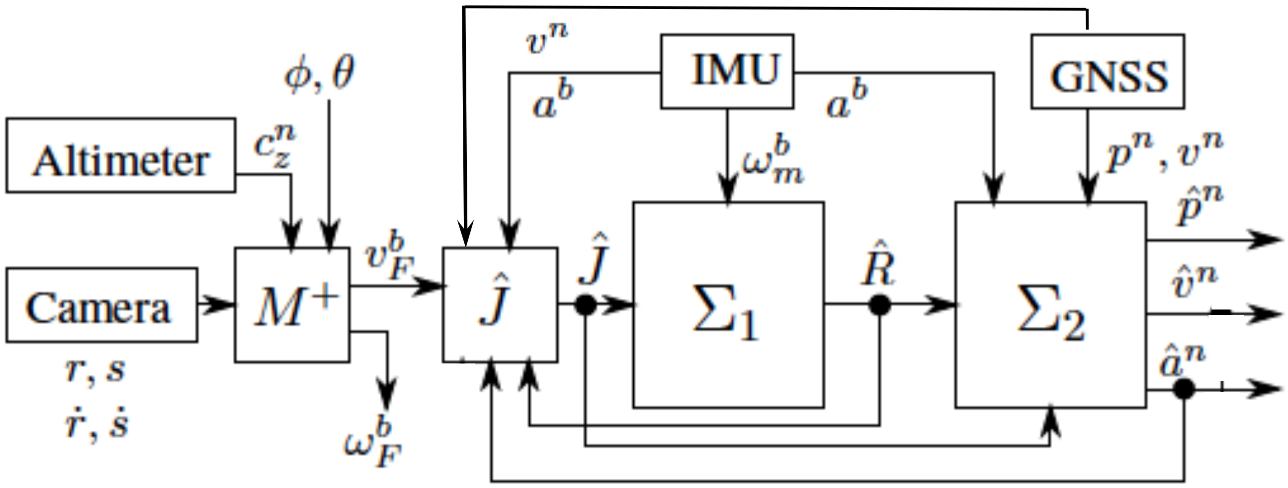

The origin of the feedback interconnection Σ_1–Σ_2 (feedback from estimated NED acceleration a^n) is GES if the roll and pitch angles in the M-matrix are auxiliary signals typically obtained by:

1. Mapping the BODY accelerations to roll and pitch angles (static solution)
2. Inclinometers for auxiliary roll and pitch measurements (sensitive to large accelerations)

If we feed the roll and pitch angles estimates from the rotation matrix attitude observer Σ_1 back to the M-matrix this introduces a hard nonlinearity. For this case, we have shown that the resulting origin of Σ_1 is ULES and Σ_2 is GES.

Fusini, L. T. I. Fossen and T. A. Johansen. Nonlinear Camera-Based INS for Fixed-Wing UAV using the eXogenous Kalman Filter. Ch. 2 in "Sensing and Control for Autonomous Vehicles: Applications to Land, Water and Air Vehicles” (T. I. Fossen, K. Y. Pettersen and H. Nijmeijer, Eds.). Springer, 2017.

Experimental Results

Test performed at Eggemoen on
6 February 2015

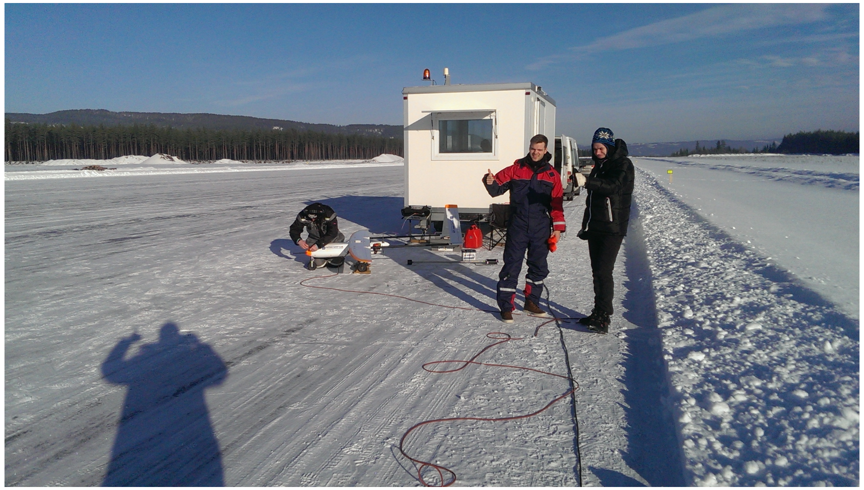

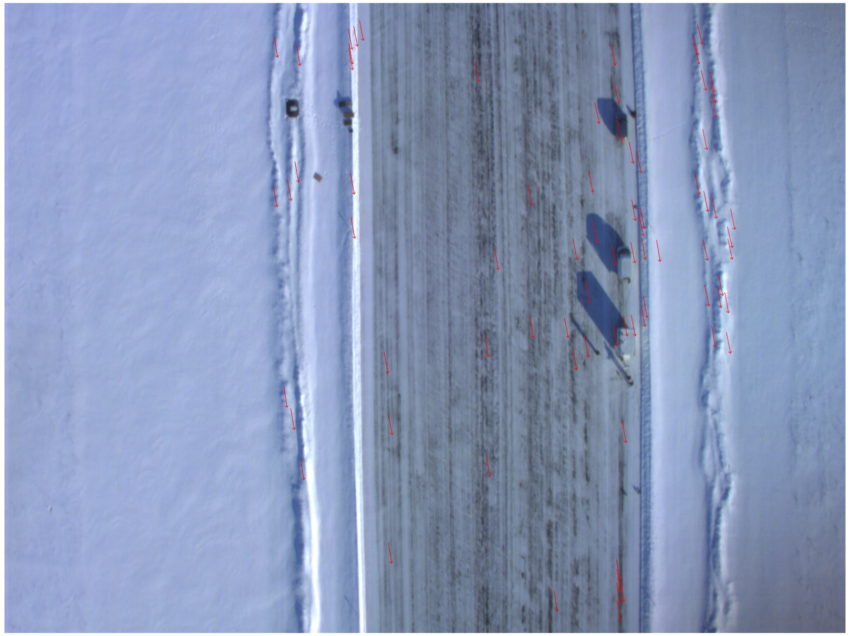

Experimental Results: Comparison of Attitude Estimator Methods

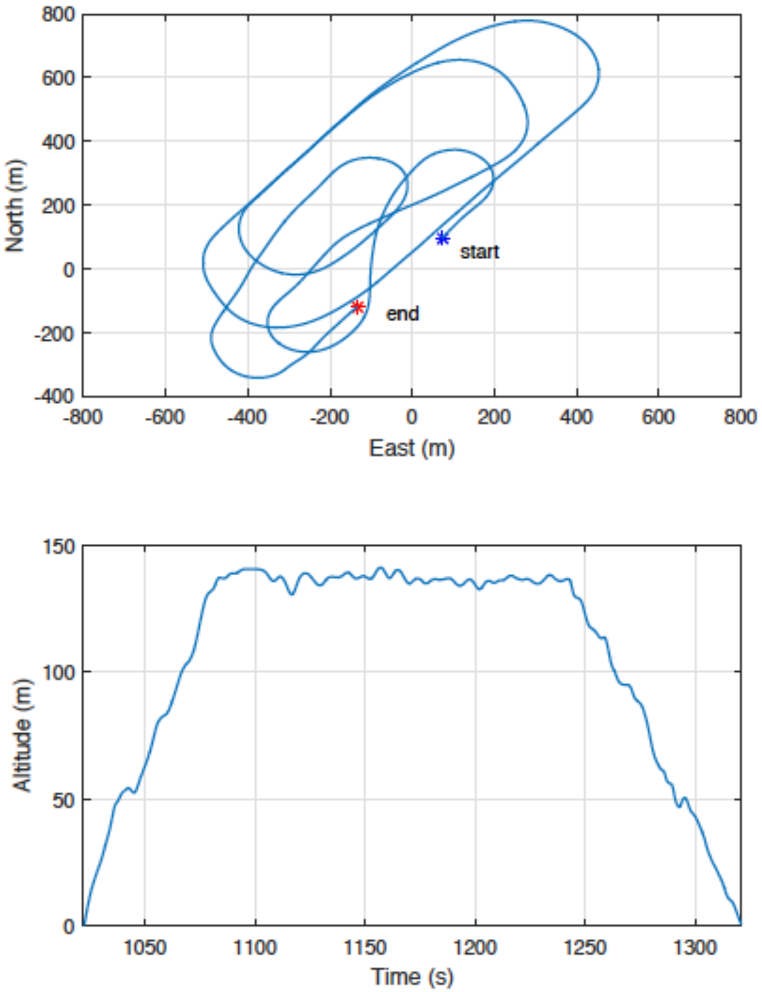

Fig. 5. Position on the N-E plane and altitude, as output by the EKF, used as reference. The blue and red stars indicate the start and end of the data set, respectively.

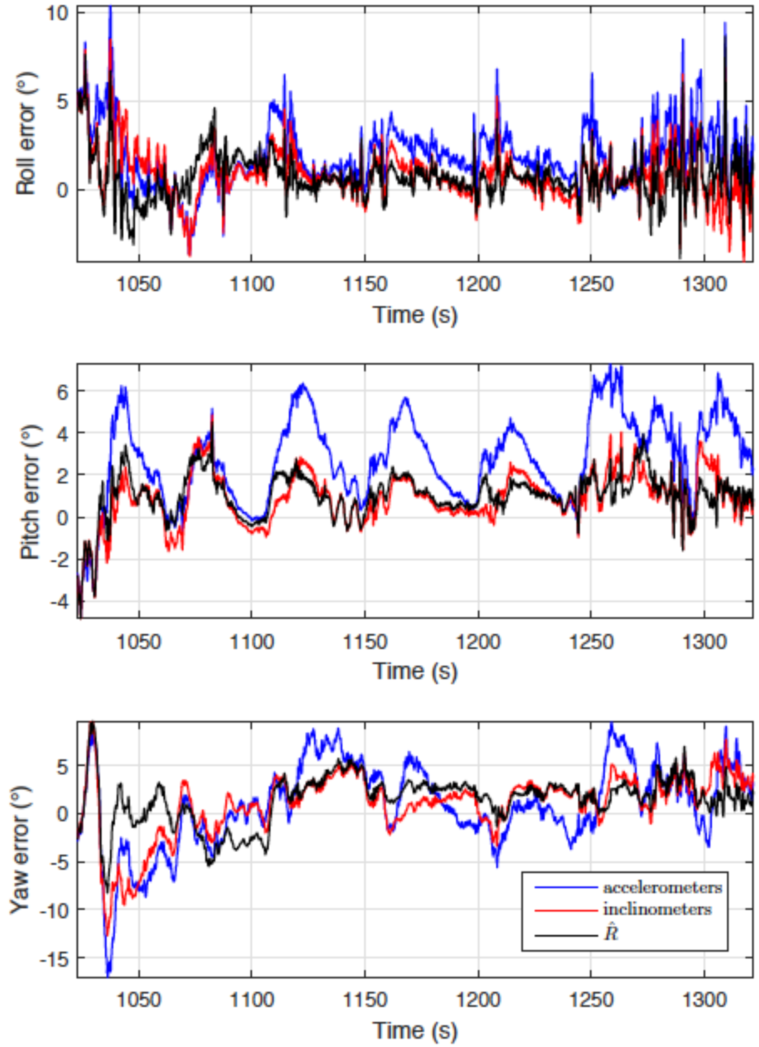

Fig. 6. A comparison of the attitude error from the three methods.

Fusini, L. T. I. Fossen and T. A. Johansen. Nonlinear Camera-Based INS for Fixed-Wing UAV using the eXogenous Kalman Filter. Ch. 2 in "Sensing and Control for Autonomous Vehicles: Applications to Land, Water and Air Vehicles" (T. I. Fossen, K. Y. Pettersen and H. Nijmeijer, Eds.). Springer, 2017.

Experimental Results: Validation of Nonlinear Observer against Autopilot EKF

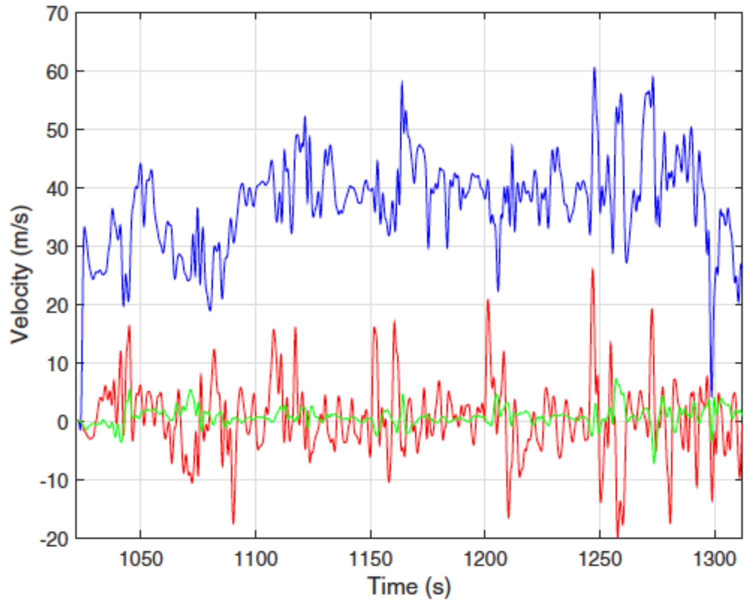

Fig. 4. Body-fixed velocity in the x, y, and z axis (blue, red, and green, respectively) calculated via machine vision.

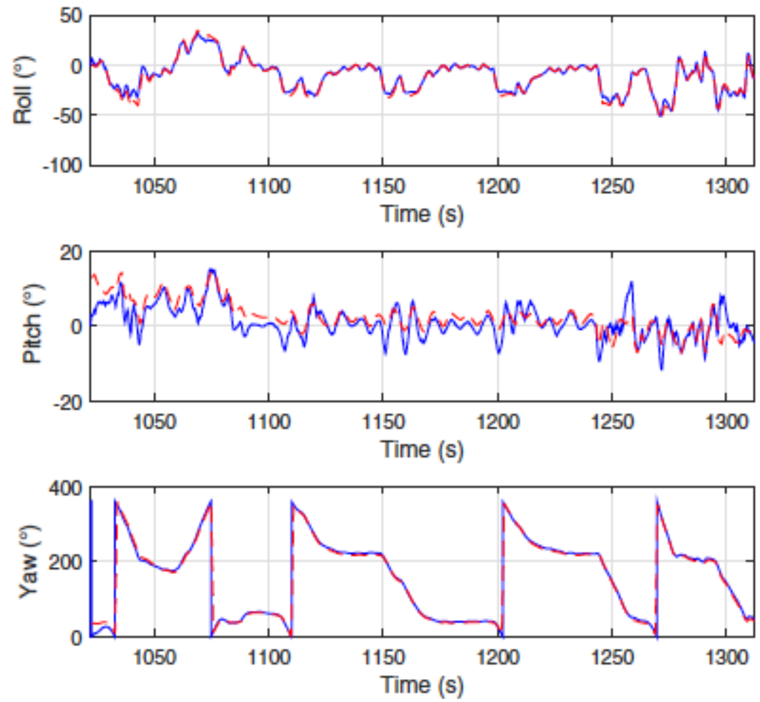

Fig. 5. Estimated (blue, solid) and EKF (red, dashed) attitude.

L. Fusini, J. Hosen, H. H. Helgesen, T. A. Johansen, T. I. Fossen (2015). Experimental Validation of a Uniformly Semi-globally Exponentially Stable Nonlinear Observer for GNSS- and Camera-aided Inertial Navigation, *International Conference on Unmanned Aircraft Systems (ICUAS'15)*, 9-12 June 2015, Denver, CO.

Continuous Epipolar Optical Flow (CEOF) Observer

The origin of Σ_1–Σ_2 is GES as long as the gyro bias is known

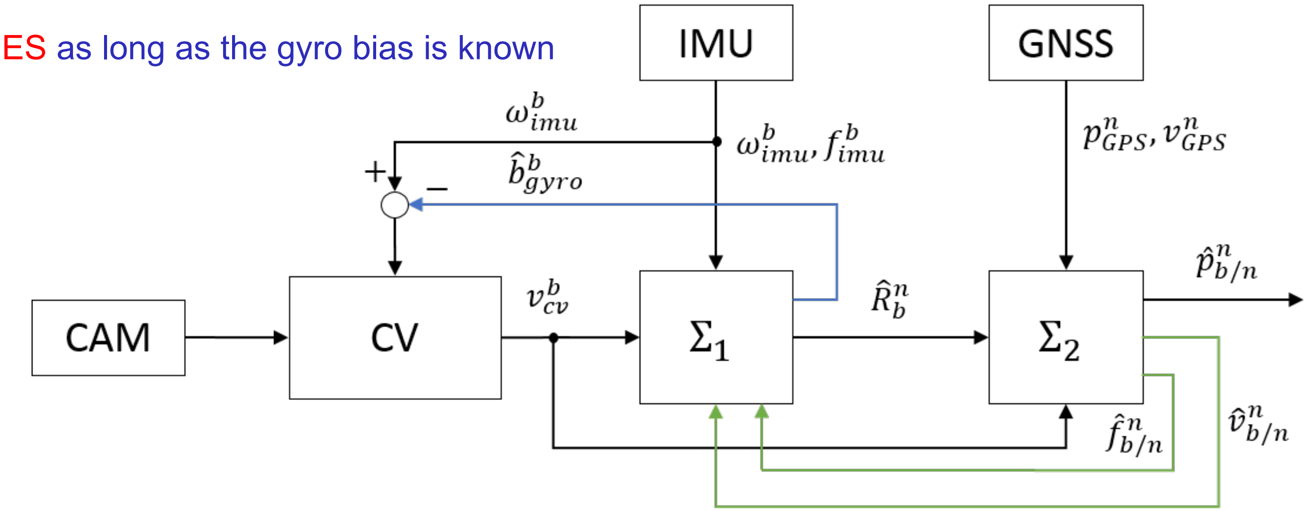

Do not need roll angle φ and pitch angle θ nor attitude h to compute the transformation matrix CV

Epipolar geometry is the geometry of stereo vision. When two cameras view a 3-D scene from two distinct positions, there are a number of geometric relations between the 3-D points and their projections onto the 2-D images that lead to constraints between the image points.

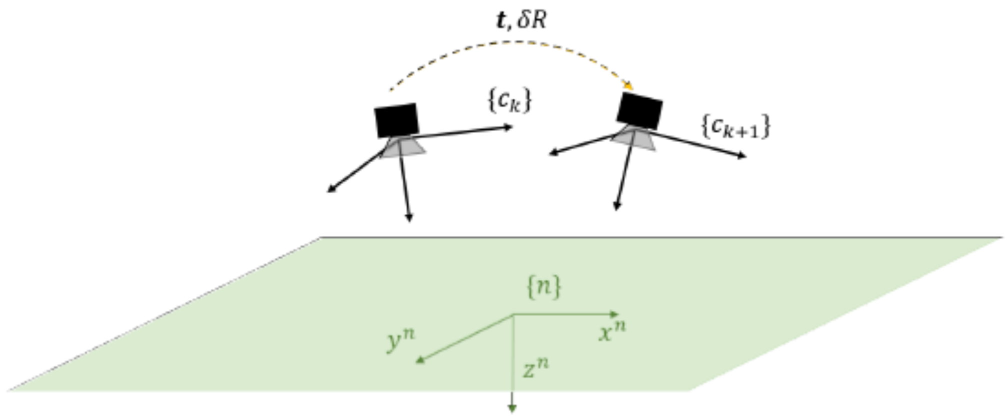

Figure 3.10: With epipolar geometry it is possible to find a dimensionless translation t and the relative rotation, δR, from time t_k to t_{k+1} without any prior information about the structure.

Hosen, J., H. H. Helgesen, L. Fusini, T. I. Fossen and T. A. Johansen. Vision-aided Nonlinear Observer for Fixed-wing Unmanned Aerial Vehicle Navigation. *Journal of Guidance, Control, and Dynamics*, Vol. 39, No. 8 (2016), pp. 1777-1789

Continuous Epipolar Optical Flow (CEOF) Observer

$$\Sigma_1 \begin{cases} \dot{\hat{R}}_b^n = \hat{R}_b^n S(\omega_{\text{imu}}^b - \hat{b}_{\text{gyro}}^b) + \sigma K_P \hat{J} \\ \dot{\hat{b}}_{\text{gyro}}^b = \text{Proj}(\hat{b}_{\text{gyro}}^b, -k_I \text{vex}(\mathbb{P}_a(\hat{R}_s^T K_P \hat{J}))) \end{cases}$$

$$\hat{J}(v_{\text{cv}}^b,\ \hat{v}_{b/n}^n, f_{\text{imu}}^b, \hat{f}_{b/n}^n, \hat{R}_b^n) := \hat{A}_n A_b^T - \hat{R}_b^n A_b A_b^T$$

$$A_b := [f_{\text{imu}}^b,\ f_{\text{imu}}^b \times v_{\text{cv}}^b,\ f_{\text{imu}}^b \times (f_{\text{imu}}^b \times v_{\text{cv}}^b)]$$

$$\hat{A}_n := [\hat{f}_{b/n}^n,\ \hat{f}_{b/n}^n \times \hat{v}_{b/n}^n,\ \hat{f}_{b/n}^n \times (\hat{f}_{b/n}^n \times \hat{v}_{b/n}^n)]$$

$$\Sigma_2 \begin{cases} \dot{\hat{p}}_{b/n}^n = \hat{v}_{b/n}^n + K_{pp}(p_{\text{GNSS}}^n - \hat{p}_{b/n}^n) + K_{pv}(v_{\text{GNSS}}^n - \hat{v}_{b/n}^n) \\ \dot{\hat{v}}_{b/n}^n = \hat{f}_{b/n}^n + g^n + K_{vp}(p_{\text{GNSS}}^n - \hat{p}_{b/n}^n) + K_{vv}(v_{\text{GNSS}}^n - \hat{v}_{b/n}^n) \\ \dot{\xi} = -\sigma K_P \hat{J} f_{\text{imu}}^b + K_{\xi p}(p_{\text{GNSS}}^n - \hat{p}_{b/n}^n) + K_{\xi v}(v_{\text{GNSS}}^n - \hat{v}_{b/n}^n) \\ \hat{f}_{b/n}^n = \hat{R}_b^n f_{\text{imu}}^b + \xi \end{cases}$$

$$\text{CV} \begin{cases} v_{\text{cv}}^b = \text{sign}(v_x) \frac{v_e}{\|v_e\|}, \quad v_x \neq 0 \\ v_e = [1, (A^+ b)^T]^T \\ [c_{x,j}, c_{y,j}, c_{y,j}]^T = u_j^c \times \left(\dot{u}_j^{cT} + \left[\omega_{\text{imu}}^b - \hat{b}_{\text{gyro}}^b \right]_\times u_j^c \right) \end{cases}$$

$$v_{c/n}^c = v_x [1, (A^+ b)^T]^T$$

$$A = \begin{bmatrix} c_{y,1} & c_{z,1} \\ \vdots & \\ c_{y,N} & c_{z,N} \end{bmatrix}$$

$$b = - \begin{bmatrix} c_{x,1} \\ \vdots \\ c_{x,N} \end{bmatrix}$$

$$[c_{x,j}, c_{y,j}, c_{z,j}]^T = u_j^c \times \left(\dot{u}_j^{cT} + \left[\omega_{c/n}^c \right]_\times u_j^c \right)$$

Hosen, J., H. H. Helgesen, L. Fusini, T. I. Fossen and T. A. Johansen. Vision-aided Nonlinear Observer for Fixed-wing Unmanned Aerial Vehicle Navigation. *Journal of Guidance, Control, and Dynamics*, Vol. 39, No. 8 (2016), pp. 1777-1789

Experimental Testing

Hosen, J., H. Helgesen, L. Fusini, T. I. Fossen and T. A. Johansen. A Vision-aided Nonlinear Observer for Fixed-wing UAV Navigation. Proceedings of the AIAA SciTech'16 San Diego, California, USA, 4-8 Jan 2016

Experimental Results

Ref = Extended Kalman filter
NoCV = Nonlinear observer without computer vision
GTOF = Ground Truth Optical Observer
CEOF = Continuous Epipolar Optical Flow Observer

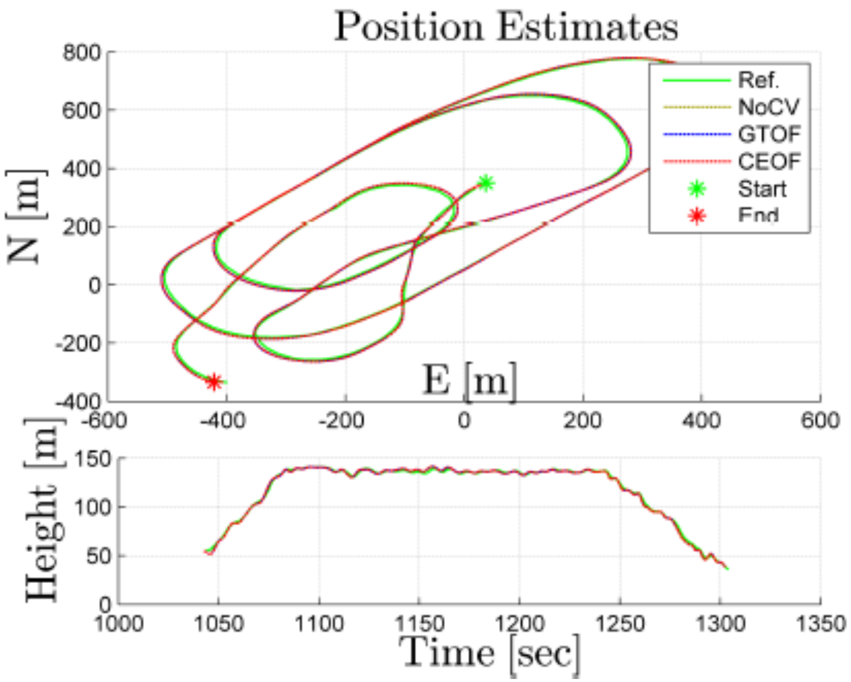

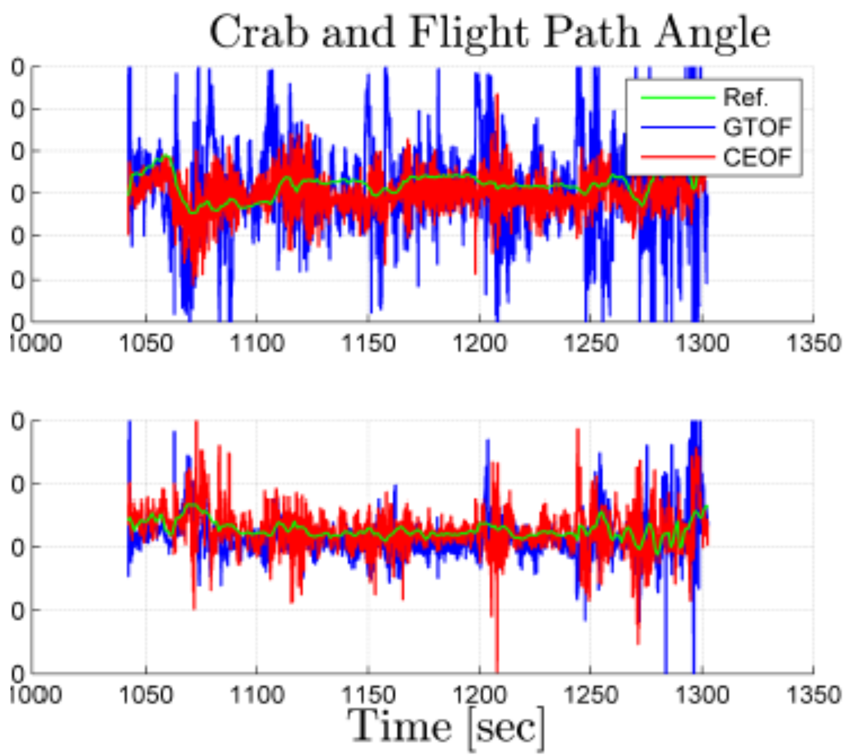

Experimental Results

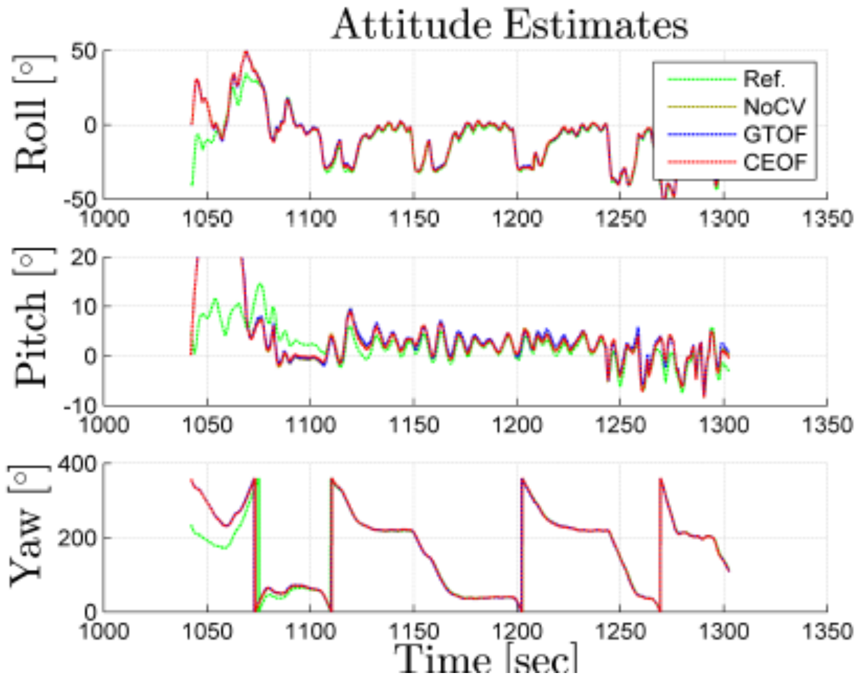

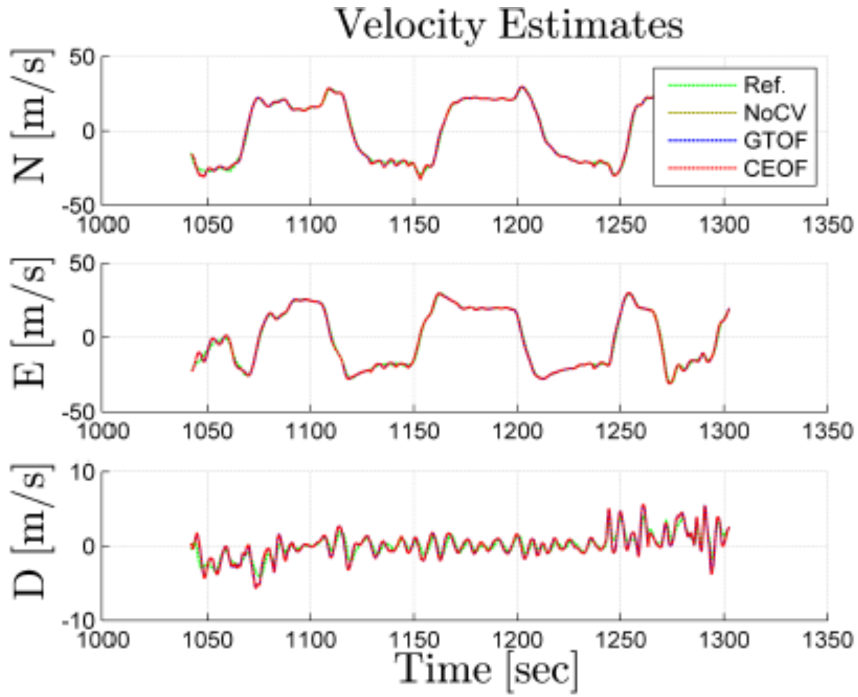

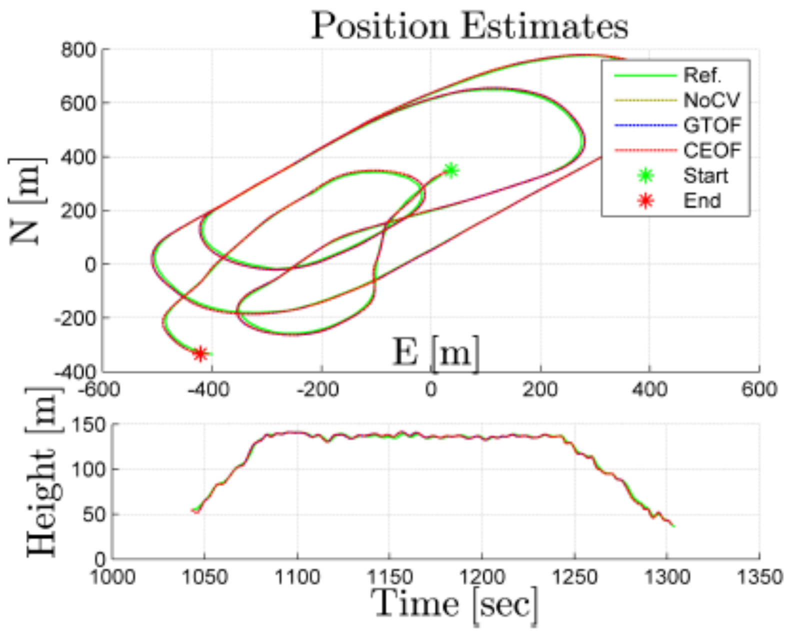

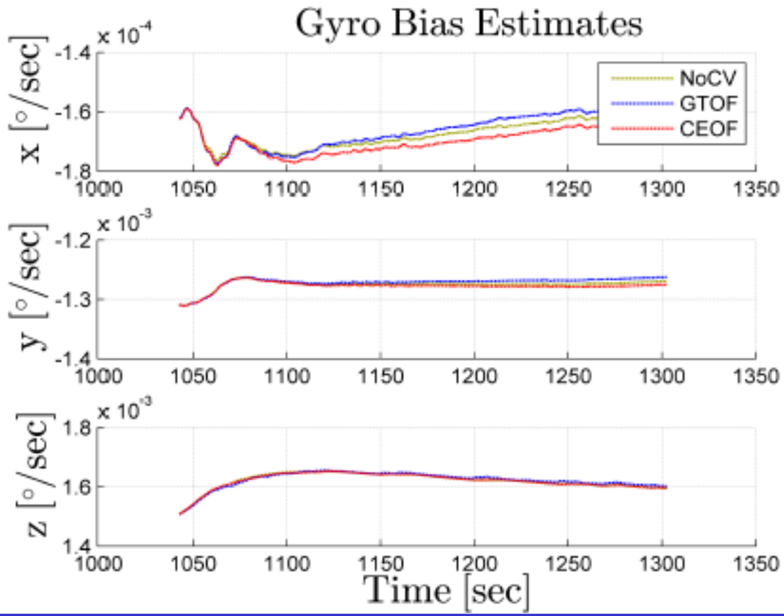

Concluding Remarks

A nonlinear observer framework has been developed for strapdown INS, which can replace the EKF without performance degradation. New observer tool: XKF

Explicit stability requirements for semiglobal and global exponential stability (GES) have been derived (not available when using the EKF). This gives robustness guarantees and tuning rules for the convergence rate of the estimates.

Compensation of delayed GNSS measurements for high-speed applications such as UAVs.

The nonlinear observer has a significant smaller computational footprint than the EKF. It is tailor made for low-cost embedded systems using MEMS sensors.

A discrete-time version, which can can handle sensors with different measurement frequencies, has been developed.

Bryne, T. H., R.H. Rogne, J.M. Hansen, N. Sokolova, T. A. Johansen and T. I. Fossen. Nonlinear Observers for Integrated INS/GNSS Navigation – Implementation Aspects. *IEEE Control Systems Magazine*, 2017

We are currently developing a Matlab toolbox and C++ library for effective implementation.


PhD Candidates
PostDocs
Thank you for your attention